

QGP in Quark Stars

A thesis submitted to the
University of Calicut in partial fulfilment of the
requirements for the award of the Degree of

DOCTOR OF PHILOSOPHY

under the Faculty of Science

by

Sineeba Ramadas



Department of Physics
University of Calicut
Kerala, India
April 2014

CERTIFICATE

Certified that this thesis entitled **QGP in quark stars** submitted by **Ms. Sineeba Ramadas** for the award of the degree of Doctor of Philosophy of the University of Calicut requires no revision as per the reports of the thesis examiners. Hence it may be submitted in the present form without any revision.

V. M. Bannur

Research Supervisor

University of Calicut

July 2015

CERTIFICATE

Certified that this thesis entitled **QGP in quark stars** is a bonafide record of research work done by **Ms. Sineeba Ramadas**, under my guidance for the award of the degree of Doctor of Philosophy of the University of Calicut and that no part of this thesis has been presented elsewhere for the award of any degree, diploma or other similar title.

V. M. Bannur

Research Supervisor

University of Calicut

March 2014

DECLARATION

I declare that the work presented in this thesis is based on the original work done by me under the guidance of Dr. V. M. Bannur, Department of Physics, University of Calicut and has not been included in any other thesis submitted previously for the award of any degree either to this university or to any other university/institution

Sineeba Ramadas

University of Calicut

March 2014

ACKNOWLEDGEMENTS

I thank my research advisor, Dr.Vishnu M. Bannur, for suggesting the problem, for his guidance and for providing the freedom to pursue the problem in my own way.

I thank Sajin Koroth of IIT Madras for taking time out of his busy life to help obtain journal papers, easy. I thank my friends, teachers and non - teaching staff at the Department of Physics for their constant encouragement and support through the years.

I express my gratitude to the Council of Scientific and Industrial research (CSIR), NewDelhi for providing financial assistance to carry out this research work.

Sineeba Ramadas

Then even nothingness was not, nor existence,
There was no air then, nor the heavens beyond it.
What covered it? Where was it? In whose keeping
Was there then cosmic water, in depths unfathomed?

Naasadiiya Suktha (Rigveda)

Contents

| | | |
|----------|---|-----------|
| 1 | Introduction | 7 |
| 1.1 | A Brief History Of Elementary Particle Physics | 7 |
| 1.2 | Discovery Of Asymptotic Freedom And The Principle Of Quark Confinement | 10 |
| 1.3 | The Quark Gluon Plasma (QGP) | 15 |
| 1.4 | Compact Stars With QGP In The Interior - Quark Stars / Hybrid Stars | 22 |
| | References | 28 |
| 2 | The QCD Phase diagram | 32 |
| 2.1 | Chiral symmetry restoration - a key feature of hot/dense QCD | 32 |
| 2.2 | The time line of QCD phase diagram | 38 |
| | References | 48 |
| 3 | The equation of state for SCQGP within a quark star and the Mass-Radius relationship | 51 |
| 3.1 | Introduction | 51 |
| 3.2 | Coupling strength and equation of state of QGP . . . | 53 |

| | |
|---|-----------|
| 3.3 The mass - radius relationship | 58 |
| References | 61 |
| 4 Radial oscillations and stability of quark stars with strongly coupled QGP in their interior | 63 |
| 4.1 Introduction | 63 |
| 4.2 Normal radial modes of quark stars in the SCQGP model | 65 |
| 4.3 Normal mode eigenfunctions of the radial modes and the energy stored in the pulsations | 70 |
| 4.4 Damping of pulsations by non-equilibrium processes . | 74 |
| References | 83 |
| 5 Conclusion | 85 |
| References | 90 |

List of Figures

| | | |
|-----|--|----|
| 2.1 | The naive phase diagram of QCD matter by Cabibbo and Parisi | 38 |
| 2.2 | A more complex phase diagram for QCD matter con- ceived by G.Baym in 1982 | 39 |
| 2.3 | A recent QCD phase diagram by Fukushima and Hat- suda | 40 |
| 3.1 | Equations of state for quark matter - A comparison be- tween SCQGP EOS evaluated for $B^{1/4} = 200$ MeV and the MIT BagModel EOS for non-interacting quarks with $m_u = m_d = 0, m_s = 150$ MeV and $B^{1/4} = 145$ MeV. | 57 |
| 3.2 | Mass- radius relationship for quark stars - A compar- ison between SCQGP EOS evaluated for $B^{1/4} = 200,$ 210, 220 MeV and the MIT BagModel EOS for non- interacting quarks with $m_u = m_d = 0, m_s = 150$ MeV and $B^{1/4} = 145$ MeV. | 59 |

| | | |
|-----|--|----|
| 3.3 | Mass sequences - A comparison between SCQGP EOS evaluated for $B^{1/4} = 200, 210, 220$ MeV and the MIT BagModel EOS for non-interacting quarks with $m_u = m_d = 0, m_s = 150$ MeV and $B^{1/4} = 145$ MeV. | 60 |
| 4.1 | (a) Oscillation periods (τ), calculated for the SCQGP EOS, as a function of central energy density (ϵ_c) for the fundamental mode | |
| | (b) For the first excited mode | 68 |
| 4.2 | (a) A comparison of oscillation periods (τ), calculated for the SCQGP EOS and the MIT BagModel EOS, as a function of stellar mass M for the fundamental mode. | |
| | (b) For the first excited mode | 69 |
| 4.3 | (a),(b),(c) The ‘relative eigenfunctions’ ξ/r , for the SCQGP EOS, plotted against the ‘relative radius’ r/R for the fundamental ($n=0$), first ($n = 1$) and second ($n = 2$) excited modes respectively. | 71 |
| 4.4 | The variation in the adiabatic index γ with energy density ϵ for the SCQGP equation of state with bag parameter $B^{1/4} = 210$ MeV | 72 |

4.5 (a) The neutrino luminosities (L), in the fundamental mode for SCQGP stars with bag parameter $B^{1/4} = 210 MeV$, as a function of time. The normalization parameter $\Delta = 0.01$.
(b) The temporal evolution of pulsation energy in the fundamental mode for SCQGP stars with bag parameter $B^{1/4} = 210 MeV$, as a function of time. 81

List of Tables

| | |
|---|----|
| 3.1 The limiting mass (M_{max}) of quark stars in the SC-QGP model for different B values. The corresponding radius (R), central energy density (ϵ_c) and quark number density (n_c) are given | 60 |
|---|----|

Chapter 1

Introduction

1.1 A Brief History Of Elementary Particle Physics

The discovery of the electron by J.J Thompson in 1897, using a simple particle accelerator - a cathode-ray tube - set the stage for modern particle physics. Electrons are elementary particles within the current experimental resolution. The proton and neutron were discovered subsequently and initially regarded as elementary particles. But soon there was a proliferation in the inventory of the so called elementary particles. The study of cosmic rays led to the discovery of muons in 1937, pions and strange particles followed a decade later. In the 1950's, after world war II, the focus of particle physicists shifted from cosmic rays to man-made particle accelerators - a transition from *particle hunters to particle farmers*. The use of particle accelerators with bubble chambers revealed a great number of new particles, including mesons of spin higher than zero and baryons of spin higher than half with various values for

charge and strangeness. All these new particles, generically called hadrons, though unstable, exhibit behaviour broadly similar to protons and neutrons. So now physicists had to deal with dozens of these hadrons, including the nucleons, which transformed to each other in various befuddling ways. Instead of nuclear force, the interaction between hadrons came to be known by a new name, the strong interaction.

The rapidly multiplying number of hadrons clearly indicated that they could not all be elementary. In the early 1960's Murray Gell-Mann and George Zweig independently put forth the quark model as a step towards a classification scheme based on certain regularities in the observed spectra of hadrons. According to the quark model all known hadrons are constituted of much more fundamental particles, which Gell-Mann called "quarks" and which came in three flavors - the up, down and strange (later charm, top and bottom quarks were added to the model)- SU(3) being the relevant symmetry group [1, 2, 3]. Baryons are composed of three quarks and mesons comprise a quark anti-quark pair. The observed patterns in masses, lifetimes, spins of the known baryons and mesons fell into place once they were assumed to have a quark substructure. The quark model gained strength by the discovery of the Ω^- particle belonging to the baryon decuplet, as predicted by the model. Quarks being fermions, in order that the Pauli principle is not violated, it was proposed by Greenberg, Han, Nambu [4, 5] that the quarks be endowed with an additional quantum number, which was later named the quark 'color' (The introduction of color as a new degree of freedom was

necessitated by the discovery of Δ^{++} particle with a substructure involving identical u quarks). Since a baryon is composed of three quarks it is quite natural to let color degrees of freedom take on three different values or we can say that each quark of a particular flavor comes in any of the three colors, say red, green or blue. Again the $\pi^0 \rightarrow 2\gamma$ decay rate is found to support the assignment of three colors to each flavor of quark. All observed hadrons are color neutral.

Despite its power to predict the existence of new particles the quark model did not receive a warm response from theorists at the time. The reason was that quarks were never detected in isolation. Even Gell-Mann regarded quarks to be mere mathematical constructs rather than a physical reality. The first experimental evidence for quarks as the real dynamical constituents of hadrons came from the deep inelastic electron-proton scattering experiments performed at the Stanford Linear Accelerator Center (SLAC) in 1968. The scattering cross-sections gave evidence of elastic scattering from point like objects inside the proton [6, 7]. The experimental results at SLAC could be explained only if quarks inside a proton are nearly free, subject to no force, as was proposed by Feynman (He used the name 'partons' for the proton constituents instead of quarks) [8, 9]. Now, there arose a paradox. The strong interaction is powerful enough to permanently confine quarks within hadrons (isolated quarks are never seen) but Feynman's suggestion requires the interaction to be weak enough at short distances so that quarks behave as if they are free particles. A solution to the paradox was provided subsequently by David Gross, Wilczek and Politzer.

The theory of strong interactions was developed in the 1970's as a generalization of the existing gauge theory of electromagnetic interaction - quantum electrodynamics (QED). In the electromagnetic case the force carriers are massless vector bosons, the photons. Analogously in the case of strong interactions the corresponding massless vector gauge bosons are called the gluons. Now the color symmetry is an exact $SU(3)$ symmetry and the gluons form an $SU(3)$ color octet. The fundamental difference between the theory of strong interaction which came to be called quantum chromodynamics (QCD) and QED is that in QCD the generators of the symmetry do not commute with each other. The theory is therefore a non-Abelian gauge field theory, the prototype of which is the Yang-Mills field. Non-Abelian gauge field theories have some peculiar properties one of which proved to provide the solution to the paradox posed by the SLAC experiment.

1.2 Discovery Of Asymptotic Freedom And The Principle Of Quark Confinement

One of the unique properties of non-abelian gauge theories and hence QCD is that they are asymptotically free. Thus for QCD, as the energy momentum transfer increases the effective interaction between quarks decreases and as these variables tend to infinity, the theory approaches a free field theory. This property is called asymptotic freedom as discovered by David Gross, Wilczek and Politzer [10, 11, 12, 13]. The asymptotic freedom is a result of the anti-

screening of color charge. Since the gluon fields themselves have color and hence have self coupling, a bare color charge centered at origin gathers in space a thundercloud of gluons. Thus as one tries to find the bare quark by moving up closer through the gluonic cloud the color charge appears smaller and smaller. As a consequence, with decrease in the typical length scale or with increase in the energy scale, the coupling strength decreases in QCD. This explains the SLAC results where quarks behave as if they are free particles, though they are indeed strongly interacting and ultimately confined. Asymptotic freedom established QCD as the fundamental theory of strong interactions.

Since the strong coupling constant (α_s) becomes small at short distances/ high momentum transfers, the interactions between quarks and gluons can be treated using perturbation theory. In field theories, the Feynman diagrams with closed loops corresponding to the quantum corrections, calculated in perturbation theory have ultraviolet divergences originating from the intermediate virtual states with high momenta. Renormalization is the procedure through which all the divergences arising from the Feynman diagrams at all orders are absorbed into a redefinition of fields masses and coupling constants. Gerard 't Hooft proved the renormalizability of the whole family of Yang-Mills theories and hence QCD [14, 15]. In the framework of perturbative QCD (pQCD) the renormalized effective coupling constant or the running (scale dependent) coupling constant is expressed as a function of μ which is the energy scale at which the divergences are renormalized. When one takes μ close to the scale

of the momentum transfer Q then $\alpha_s(\mu^2 = Q^2)$ and gives the effective strength of coupling for the process. The coupling satisfies the following renormalization group equation:

$$\mu^2 \frac{d\alpha_s}{d\mu^2} = \beta(\alpha_s) = -(\beta_0 \alpha_s^2 + \beta_1 \alpha_s^3 + \dots) \quad (1.1)$$

where $\beta_0 = \frac{1}{4\pi}(11 - \frac{2}{3}n_f)$ is referred to as the one loop beta-function coefficient, β_1 is the two loop beta-function coefficient and so on and n_f is the number of quark flavors. With $n_f = 3$ in the one loop approximation an exact analytic solution exists for eqn(1) and is given by

$$\alpha_s(\mu^2) = \frac{1}{\beta_0^2 \ln(\frac{\mu^2}{\Lambda^2})} \quad (1.2)$$

Here Λ is a constant of integration which gives the scale at which the perturbatively defined coupling constant diverges. Λ therefore corresponds to the non-perturbative scale of QCD. It is called the QCD scale parameter, to be determined from experiments. The equation (1.2) clearly indicates that at large momentum transfers, the coupling strength $\alpha_s \rightarrow 0$. The quarks therefore behave as if they are free particles(asymptotic freedom). On the other hand, at low momentum transfers or equivalently, larger distances, $Q \sim \Lambda$, α_s becomes quite large and the perturbation theory is no longer reliable. This behaviour may be linked to the confinement of quarks and gluons within hadrons and is known by the name ‘infrared slavery’. Since QCD in the non perturbative regime is intractable analytically, phenomenological models are employed in order to compute the various properties of hadrons.

At small distances where the coupling constant which determines the strength of quark-gluon interaction is small, it is expected that the quark-quark interaction should bear some resemblance to electron-electron interaction. According to phenomenological potential models, at small distances the dominant contribution to the qq interaction is the one gluon exchange interaction. The one gluon exchange potential (OGP) is mostly of the Coulomb type and very similar to one photon exchange potential between electrons, gluon and photon being both massless. The main difference apart from the difference in coupling strength is a numerical factor (generally called the Casimir factor), arising from the non-abelian nature of the colored gluons. Accordingly the strength of quark-antiquark interaction in a color singlet state is given by $-\frac{4\alpha_s}{3}$ and that for quark-quark interaction in a color singlet state by $-\frac{2\alpha_s}{3}$ (The analogous strengths in the electron-positron and electron-electron case are $-\alpha$ and $+\alpha$ respectively, α being the fine structure constant).

The long distance confining potential does not follow directly from field theory. A number of possible options for the potential at large distances is available phenomenologically, subject to the constraint that they are able to reproduce the hadronic masses. A linear confining potential is quite plausible and the most commonly used. The total interaction potential for quarks is most often written as the sum of the Coulombic one gluon exchange potential and the linear confining potential,

$$V(r) = \frac{C\alpha_s}{r} + Kr \quad (1.3)$$

Here C is the color Casimir factor. The constant K is referred to as the string tension. The lines of force of the color field pulled together by the gluon-gluon interaction can be imagined to take the form of a tube or string. If the string is pulled indefinitely then the stored energy reaches a point such that it is energetically more favourable to break into two short strings, say by creating a new quark-antiquark pair. A potential of this form was pioneered by the Cornell group and is called the Cornell potential [16, 17].

Another non-perturbative approach to QCD is Wilson's lattice gauge theory (LGT) [18]. In lattice QCD the 4-D space time is discretized to a lattice with quarks occupying the lattice sites and gluons, the lattice links. On a discrete space time the path integral that defines the theory becomes finite dimensional and can be evaluated utilizing the Monte Carlo methods. Lattice QCD calculations in the quenched approximation have been made to simulate the heavy quark-antiquark potential for a color singlet, and the results, interestingly, show a linearly rising confining term in the potential. The potential computed on the lattice was found to be very much in agreement with a Coulomb + linear potential (the Cornell potential) [19]. The lattice studies carried out so far hence leave little doubt that the quarks are indeed confined, though a first principle derivation of confinement is yet to be done.

1.3 The Quark Gluon Plasma (QGP)

In 1965 almost a decade before the discovery of asymptotic freedom Hagedorn had predicted a limiting temperature for "strong interactions" [20, 21]. Analysing the high energy hadronic collisions using a bootstrap statistical model (BSM) he found that the hadronic mass spectrum shows the following asymptotic behaviour- it grows exponentially with increasing mass. He proposed that as the energy of collision becomes large the temperature tends to a finite limit which is the highest attainable temperature with a numerical value of about 160 MeV ¹. The existence of an energy independent highest temperature is a consequence of the exponentially growing mass spectrum. As more and more energy is pumped into the system it is consumed to excite resonances, create more and more particles rather than increasing the kinetic energy of existing particles. Thus in the limit the kinetic energy per particles tends to remain a constant, the temperature reaches the highest possible value. But the above conclusions were reached by assuming hadrons to be point particles devoid of a finite size.

Quark models visualize hadrons as having a finite size with quarks as their fundamental constituents. With the advent of asymptotic freedom quarks were known to interact weakly in close proximity. Relying on these ideas in 1975 Cabibbo and Parisi in their seminal paper entitled 'Exponential hadronic spectrum and quark liberation' [12] proposed that the Hagedorn temperature was not a high

¹Here and throughout the thesis natural units are employed, else otherwise stated explicitly.

temperature limit, rather it is the critical temperature for phase transition to underlying quark gluon matter. The picture is clear within the MIT bag model - the model ideates hadrons to be bubbles of perturbative vacuum to which quarks are confined but in the interior of which quarks can move about freely [22]. The perturbative vacuum is an excited state, with an energy density B (called the bag constant), above normal QCD vacuum. In conformity with the Hagedorn spectra, the bag model gives an exponential mass spectrum which follows from a particular feature of the model - the mass of the bag is proportional to the time averaged volume. With increasing energy density the bags cluster and overlap with each other. The component quarks find in their vicinity more and more quarks, thereby loosing their sense of belonging to a particular bag. The model therefore provides an intuitive picture of a deconfinement transition of hadronic matter to quark gluon matter wherein the quarks interact weakly owing to asymptotic freedom.

Concurrent to Cabibbo and Parisi, Collins and Perry suggested that super dense matter which should exist in the neutron star cores, exploding black holes, early big bang universe essentially comprises a quark soup [13]. For instance within a neutron star where the central density could be as high as 10 times the normal nuclear density the hadrons overlap with the fundamental quarks confusing their individuality. Quarks being asymptotically free a weakly interacting quark gluon matter is therefore expected at such high densities. They proposed that due to many body effects long range interactions are screened in such systems banishing problems arising due

to the infrared behaviour of quark confining forces. In 1978 calculations by Edward Shuryak showed that unlike virtual gluon loops in QCD vacuum which antiscreen the color charge, in real quark gluon matter the gluons screen the color charge [26]. Since this behaviour is inherent to conventional QED plasma Shuryak coined the name Quark Gluon Plasma (QGP for short) for the new deconfined phase of quarks and gluons.

There was a fervour of excitement over this new predicted phase. Could it be produced in the laboratory under controlled conditions? Heavy ion collisions with higher collision energies than ever before would be required to accomplish the feat. Since the primordial matter a few microseconds after the big bang should possibly have been a soup of quark and gluons, QGP if produced in the lab could give valuable information about the creation and evolution of the universe. The search for the phase transition from hadronic matter to quark-gluon plasma (QGP) utilizing high energy heavy ion collisions began in the mid-1980s with experiments at CERN's Super Proton Synchrotron (SPS) in Europe, and Brookhaven's Alternating Gradient Synchrotron (AGS) in the US. In 2000, the search moved onto the Relativistic Heavy Ion Collider (RHIC) at Brookhaven and later to CERN's Large hadron collider (LHC). Heavy ion collision experiments at AGS has lab energy $\sim 2-11$ GeV per nucleon pair while SPS accelerates heavy ions at lab energy ~ 200 GeV per nucleon pair. At AGS/SPS the collision experiments are fixed target experiments. RHIC/LHC are heavy ion colliders where countercirculating beams of heavy nuclei collide at huge center of mass energies. RHIC

accelerates and collides ions at center of mass energies as high as 200 GeV per nucleon pair for gold nuclei. LHC the worlds largest and highest energy - particle accelerator can accelerate and collide lead beams at extremely high center of mass energy ~ 5.4 TeV per nucleon pair.

When two heavy nuclei such as the gold nuclei are accelerated to ultra relativistic energies and then caused to make a head on collision, the nuclei become Lorentz contracted as 'pancakes'. Then the nucleon-nucleon collisions within the nucleus-nucleus collisions occur almost simultaneously and at spatial proximity thereby creating a region of very high energy density. But QGP even if created in the initial stages of such collisions, cools rapidly, by expansion and by the emission of various radiation and finally makes a phase transition to a gas of hadrons. Hence the collider experiments rely on signatures of QGP provided by theory. The most propitious signatures that provide information about QGP formation are: (1) An excess of "direct photon" production - Direct photons produced from the interaction of matter in the hot QGP phase lie in the region of photon transverse momentum p_T in the range $2 - 3$ GeV/c . The photons provide information about the properties of QGP at the time of their production. Since they are hardly absorbed by the medium they are relatively 'clean' probes of the QGP phase. (2) Strangeness enhancement - A high abundance of strangeness in the QGP drop is predicted resulting from strangeness pair production mainly due to gluon fusion process $gg \rightarrow s\bar{s}$ [23]. Therefore during hadronization processes there should be a high yield in the other-

wise rarely produced particles such as strange antibaryons.

(3) J/ψ meson suppression - If $c\bar{c}$ pair production occurs in a heavy ion collision and if the collision results in the formation of QGP then color screening in the plasma prevents the binding of charm and anticharm quarks to form J/ψ . J/ψ suppression therefore is a positive signature of QGP formation.

Though the pioneering heavy ion collisions at AGS and SPS provided an opportunity to study excited nuclear matter at high energy densities with voluminous production of various particle species no unambiguous evidence for the formation of QGP was provided. Strangeness enhancement was observed and measured for various systems in nucleus-nucleus collisions at the AGS [27] and the SPS [28, 29, 30, 31, 32] and a suppression of J/ψ [33] was measured for central collisions in nucleus-nucleus experiments at the SPS but neither AGS/SPS could provide direct evidence for QGP formation. In the RHIC heavy ion experiments, immediately after the beams collide, the energy density far exceeds the theoretical requirements for the creation of the QGP. Lattice calculations give values in the range of about 170 to 180 MeV for the critical temperature which corresponds to about 10^{12} Kelvin. One of the most remarkable observations at RHIC was a phenomenon called jet quenching which has been predicted theoretically as a possible QGP signature and which could provide a powerful new probe of QGP produced in the collisions. The collision energy at RHIC is high enough to produce the direct high-energy scattering of individual partons in the colliding nuclei. Such hard scattering events involving high momentum

transfers give rise to collimated sprays of hadrons called jets. The RHIC data shows a deficit of jets involving high p_T particles in the most central collisions [34]. The deficit of high energy jets can be attributed to the slowing down of partons as they propagate through QGP formed in the collision. The phenomena of quenching of high p_T jets gives compelling evidence that QGP is formed at the RHIC. The experiments at LHC again showed jet quenching with the high energy jets getting almost entirely dissipated, thus providing imperative evidence for the formation of QGP [35, 36].

Initially it was expected that QGP if produced in the collisions would behave like a free gas of deconfined quarks and gluons. On the contrary experiments at RHIC gave evidence that the hot and dense matter formed in collisions shows a deviation from ideal gas behaviour. The flow is similar to an ideal liquid with nearly zero viscosity. Surprisingly the experiments carried out at LHC strongly indicate that the QGP formed remains a strongly coupled, near perfect liquid even at significantly higher energies [37].

At RHIC/LHC the center of mass energy per nucleon is so high that the colliding nuclei tend to be transparent to each other. Though fragmented by the collision they essentially recede in the same directions they came in, leaving behind an excited central vacuum region low in baryon density. Therefore these collider experiments are focussed to study QGP formed at high temperatures but low net baryon densities. What about the high baryon density - low temperature regime? Cold matter at high net baryon density can be effectuated by a slow squeeze of nuclear matter which is im-

possible to enact in the lab. Therefore we turn to nature and her giant laboratories - the compact stars - where cold superdense matter and hence the presence of QGP is expected ². Compact stars are the end products of thermonuclear evolution involving massive stars. Once the nuclear fuel that 'runs' the star is exhausted the more massive stars succumb to a violent ending wherein the core collapses indefinitely. Once the core material becomes incompressible an outgoing shockwave results and there is a violent ejection of the stars' outer layers namely the supernova explosion (This is actually a naive picture of a more complex process - a controversial topic, subject to intense debate). The remaining compact remnant could be a neutron star, depending on the mass of the progenitor, supported against gravity by the neutron degeneracy pressure. But as suggested by Collins and Perry such compact remnants which admit superdense matter could be natures cache of the exotic QGP phase. Many questions arise when we consider quark matter within compact star interiors - Will there be a new class of stable compact stars - the quark stars? Is there a critical density at which the presence of QGP is expected? Will the quarks be essentially massless or instead be massive 'dressed' quarks? QGP if present, will it be an ideal gas of weakly interacting quarks or will it be in the strongly coupled phase? All these are interesting and intriguing questions and highly debated. The aim of the thesis is to fathom the presence

²Compressed baryonic matter (CBM) experiment at the Facility for antiproton and ion research (FAIR) is a future project which will explore the high density regime at moderate temperatures. This regime can be explored in heavy-ion collisions at intermediate beam energies - the colliding nuclei tend to stay with each other - with the highest baryon density reached for beam energy range between 10 and 40 GeV per nucleon. FAIR would provide beams in the energy range 2-45 GeV per nucleon.

of the exotic new phase of matter in compact stars and an attempt to address some of the debated issues.

1.4 Compact Stars With QGP In The Interior - Quark Stars / Hybrid Stars

Soon after the hadrons were conferred with a quark substructure, Ivanenkov and Kurdgelaidze hypothesised the possibility of a quark star [38]. They suggested that quark stars are the next in sequence to neutron stars, prior to black holes. In their paper published in 1965, ‘Hypothesis concerning quark stars’, they made a rough calculation of the densities at which the ‘disintegration’ process from baryons to quarks would occur. At the time, which was almost a decade before the discovery of asymptotic freedom and the advent of QCD, they had visualised the transition as similar to nuclear disintegration. Later in 1970, Itoh studied the hydrostatic equilibrium of such hypothetical stars treating quarks as a degenerate fermion gas [39]. His calculations revealed stars with equilibrium mass of the order $\sim 10^{-3} M_\odot$, far less compared to typical neutron star masses. Quark stars thus remained more or less a vague and fanciful idea until the end of the 1960s’. The discovery of asymptotic freedom of quarks led to a paradigm shift, making exotic stars comprising quark matter very much a possibility.

The question of whether the deconfined QGP would be present in compact star interiors was first considered by Baym and Chin[40]. In their paper ‘Can a neutron star be a giant MIT bag’, they consid-

ered the phase transition from neutron matter to deconfined quark matter. This was done by comparing the energy per baryon for fixed number densities in the two phases treating the quark matter phase within the MIT bag model (quarks can move about freely within the volume of dense matter but the region as a whole is color neutral). They concluded that such a phase transition would require huge densities of the order of 10 to 20 times the normal nuclear density and hence considered such a transition unlikely at relevant neutron star densities. But it was soon pointed out that such calculations are very sensitive to even small uncertainties in the chosen hypothetical equations of state for hadronic/quark matter. Based on other quark matter models - derived within QCD and consistent with the then available nuclear/ high energy physics data - Fechner and Joss showed that quarks stars are indeed possible [43]. Their studies revealed that the macroscopic properties of quark stars need not be considerably different from ordinary neutron stars.

It can be surmised that quark matter could exist within a compact star in two different forms depending on the distribution of baryon densities. One is pure quark matter devoid of baryons, which will probably occupy the core region. The other is a mixed phase where quarks and hadrons are interspersed and in phase equilibrium with each other. Compact stars with quark or mixed phase interiors are named hybrid stars. There is one more possible mode of existence of quark stars - the so called strange stars. In 1984 Witten in his seminal paper which considered the hadronization of early universe, emphasised the idea of strange quark matter being the ab-

solute ground state of hadronic matter [42]. The idea was originally proposed by Bodmer [41] and noted by several others in their work. Strange quark matter (SQM) is made up of an equal number of u, d and s quarks. The addition of strangeness lowers the stability of nuclear matter, the strange baryons being heavier than non strange baryons. The presence of strangeness in bulk quark matter stabilizes it by lowering its energy which should be attributed to the newly added Fermi well. The Fermi momenta in quark matter is of order of 300-350 MeV, which is greater than the strange quark mass. Hence it is energetically favourable for u,d quarks to undergo a flavor change to strange quarks via weak interactions. Simple calculations reveal that strange quark matter has an energy per baryon ~ 0.9 times that of two flavor u,d quark matter. The energy per nucleon of SQM therefore lies in the vicinity of ordinary nuclear matter. If it is lower than that of nuclear matter then strange quark matter would be the absolute ground state of hadronic matter, nuclear matter being a long lived metastable state. The decay of ordinary nuclei to strange matter is inhibited by the need for very high order weak interactions. If strange quark matter was indeed the ground state of hadronic matter then it implies the existence of a new class of self bound pure quark stars - the strange stars.

To distinguish between strange/hybrid stars and ordinary hadronic stars is not easy since their macroscopic properties seem to overlap. One possible feature of quark stars that can aid in their detection is the expected anomalous cooling behaviour. Neutrino emission is the primary process via which neutron stars cool during the first 10^6

years after their formation. The neutrino production via the Urca processes (simple beta decay processes) is controlled by the high density phase that exists at the core. Due to the extended degrees of freedom, quark matter has comparably higher neutrino luminosities. Hence quark stars, at a given age, should have lower surface temperatures as compared to hadronic stars. The measurement of surface temperatures of neutron stars of known age can therefore provide information about the high density phase that exists at the core. Studies along these lines has led to the detection of a potential quark star candidate - a 65 ms pulsar J0205+6449 at the center of a young supernova remnant, 3C58. 3C58 is evidently associated with supernova SN 1181, which would make it younger than the Crab Nebula. J0205+6449 is therefore one of the youngest neutron stars in the galaxy. Chandra observations of the emission from the particular neutron star gives a surface temperature well below that predicted by standard cooling mechanisms [44]. This points to enhanced neutrino production rates in the stellar interior. Therefore it is quite plausible that J0205+6449 contains some exotic phase, such as quark matter within.

Mass-radius (M-R) relationship is a key factor that gives a measure of the compactness of a star. It can therefore provide information about the nature of dense matter within. X-ray bursts that emanate from neutron stars in binary systems exhibit a number of spectroscopic phenomena that depend on the mass and radius of the neutron star. X-ray bursts are thermonuclear explosions which result from the accretion of matter on the surface of neutron stars

in binaries. Once the distance to the source star is known, using the calculated temperature (assuming black body emission) and measured flux, it is possible to set up constraints for the mass-radius relationship. Based on the M-R relationship thus obtained for neutron stars in the binaries 4U1608-248, EXO 1745-248 and 4U1820-30, Ozel et al. [45] calculated the pressure of dense matter above nuclear saturation density. The pressure was found to be lower than that predicted by pure nucleonic equations of state. This suggests that exotic matter could be present within the neutron star interiors. To pin down the equation of state at high densities we need more sensitive observational data. It is believed that future prospects such as gravitational wave detection could help probe the interiors of neutron stars. Non radial oscillations of compact stars are sources of gravitational radiation. The frequencies and damping times of the oscillation modes can be directly linked to the stellar properties such as mass, radius, rotation rate etc. The detection of the gravitational waves which damp out the oscillation, can therefore aid in obtaining valuable information about the source star. Within the next decade gravitational-wave (GW) observations by Advanced LIGO in the United States, Advanced Virgo and GEO HF in Europe, are hoped to provide new insights in this field.

Verifying and discerning the dense QGP phase in compact stars requires new efficient models and equations of state, which can predict new possible signatures for the exotic phase. In the next chapter we give a brief account of the the historical evolution of the QCD phase diagram, present the one now in vogue and discuss it with

emphasis on low temperatures and high densities. The different proposed phases at densities relevant to compact stars will be given special importance.

References

- [1] M. Gell-Mann (1964) Phys. Lett. 8, 214.
- [2] G. Zweig (1964) CERN Report No. 8182/TH 401.
- [3] G. Zweig (1964) CERN Report No. 8419/TH 412.
- [4] O. W. Greenberg (1964) Phys. Rev. Lett. 13, 598.
- [5] M. Y. Han, Y. Nambu (1965) Phys. Rev. 139, B1006.
- [6] Bloom, D. Elliott et al. (1969) Phys. Rev. Lett. 23, 930.
- [7] Breidenbach, Martin et al. (1969) Phys. Rev. Lett. 23, 935.
- [8] R.P. Feynman (1969) Phys. Rev. Lett. 23, 1415.
- [9] R.P. Feynman in *Stony Brook 1969, Proceedings, Conference On High Energy Collisions*, ed. C.N. Yang, et al, (Gordon and Breach, New York 1969), 237.
- [10] D. Gross, F. Wilczek (1973) Phys. Rev. Lett. 30, 1343.
- [11] H. Politzer (1973) Phys. Rev. Lett. 30, 1346.
- [12] D. Gross, F. Wilczek (1973) Phys. Rev. D 8, 3633.
- [13] D. Gross, F. Wilczek (1974) Phys. Rev. D 9, 980.

- [14] G.'t Hooft (1971) Nucl. Phys. B33, 173.
- [15] G.'t Hooft (1971) Nucl. Phys. B35, 167.
- [16] E. Eichten et al. (1978) Phys. Rev. D17, 3090.
- [17] E. Eichten et al. (1980) Phys. Rev. D21, 203.
- [18] K. G. Wilson (1974) Phys. Rev. D 10, 2445.
- [19] G. S. Bali (2001) Phys. Rept. 343, 1.
- [20] R. Hagedorn (1965) Nuovo Cimento Suppl. 3, 147.
- [21] R. Hagedorn, J. Ranft (1968) Nuovo Cimento Suppl. 6, 169.
- [22] A. Chodos, R. L. Jaffe, K. Johnson, C. B. Thorn, V. f. Weisskopf (1974) Phys. Rev. D 9, 3471.
- [23] J. Rafelski, B. Mller (1982) Phys. Rev. Lett. 48, 1066.
- [24] N. Cabibbo, G. Parisi (1975) Phys. Lett. B, 59, 67.
- [25] J. C. Collins, M. J. Perry (1974) Phys. Rev. Lett., 34, 1353.
- [26] E. V Shuryak (1978) Zh.E.T.F 74, 408 (Sov. Phys. JETP 47 (1978) 212).
- [27] T. Abbott et al. (1994) Phys. Rev. C 50, 1024.
- [28] T. Alber et al. (1994) Z. Phys. C 64, 195.
- [29] E. Anderson et al. (1992) Phys. Lett. B 294, 127; (1994) Phys. Lett. B 327, 433.

- [30] S. Abatzis et al. (1994) Nucl. Phys. A 566, 499c ; (1994) A 566, 491c ; (1994) A566, 225c ; (1993) Phys. Lett. B 316, 615 ; DiBari D. et al. (1995) Nucl. Phys. A 590, 307c.
- [31] J. B. Kinson et al. (1995) Nucl. Phys. A 590, 317c.
- [32] M. Gazdzicki et al. (1995) Nucl. Phys. A 590, 197c.
- [33] C. Baglin et al. (1989) Phys. Lett. B 220, 471 ; (1990) B 251, 465 ; (1991) B 262, 362; (1991) B 268, 453 ; (1991) B 270, 105.
- [34] K. Adcox et al. (PHENIX collaboration) (2002) Phys. Rev. Lett. 88, 022301; C. Adler et al. (STAR collaboration) (2003) Phys. Rev. Lett. 90, 082302.
- [35] G. Aad et al. (2010) Phys. Rev. Lett. 105, 252303.
- [36] S. Chatrchyan et al. [CMS Collaboration] (2011) Phys. Rev. C 84, 024906.
- [37] K. Aamodt et al. (ALICE Collaboration) (2010) Phys. Rev. Lett. 105, 252302.
- [38] D.D. Ivanenko, D.F. Kurdgelaide (1965) Astrophysics 1, 251.
- [39] N. Itoh (1970) Prog. Theor. Phys. 44, 291.
- [40] G. Baym, S. A. Chin (1976) Phys. Lett. B 62, 241.
- [41] A. R. Bodmer (1971) Phys. Rev. D 4, 1601.
- [42] E. Witten (1984) Phys. Rev. D 30, 272.
- [43] W. B. Fechner, P. C. Joss (1978) Nature 274, 347.

- [44] P.O. Slane, D.J. Helfand, S.S. Murray (2002) *Astrophys. J.* 571, L45.
- [45] F. Ozel, G. Baym, T. Guver, *Phys. Rev. D* (2010) 82, 101301.

Chapter 2

The QCD Phase diagram

2.1 Chiral symmetry restoration - a key feature of hot/dense QCD

Besides the deconfining transition there is another key feature concomitant with quark gluon plasma (QGP) formation. It is the chiral symmetry restoration associated with the light quark flavors. The word 'chirality' means handedness. An object is said to be 'chiral' if it is non-identical to its mirror image. The chirality of a particle is a subtle and abstract notion which is equivalent to the particles' helicity , if the particle is massless. Chirality is a Lorentz invariant i.e. a massive particle has a specific chirality. Particles can be left chiral or right chiral, defined using the eigen values of the chirality operator. For a Dirac Fermion the chirality projection operators are given by $\frac{1 \pm \gamma_5}{2}$ where γ_μ are the standard Dirac matrices and $\gamma_5 \equiv i\gamma_0\gamma_1\gamma_2\gamma_3\gamma_4$. The chirality projection operators project out the left handed and right handed states of the Fermion field,

$\psi_L = \frac{1-\gamma_5}{2}\psi$ and $\psi_R = \frac{1+\gamma_5}{2}\psi$. The total Fermion field is simply, $\psi = \psi_L + \psi_R$. If the right handed and left handed Fermions (for eg. the quarks) can make separate transformations independent of each other then the corresponding theory is said to possess chiral symmetry.

The QCD Lagrangian is given by,

$$\mathcal{L}_{QCD} = \bar{\psi}_f (i\cancel{D} - m_f) \psi_f - \frac{1}{4} F_{\mu\nu}^a F_a^{\mu\nu} \quad (2.1)$$

where ψ_f denotes the quark field and m_f denotes the quark mass, where f stands for a particular quark flavor. Here we define $\cancel{D} \equiv \gamma^\mu D_\mu$, where D_μ is a covariant derivative acting on the color triplet quark field. We have $D_\mu \equiv \partial_\mu + igA_\mu^a \lambda_a/2$. A_μ^a stands for the gluon fields, g is the dimensionless coupling constant in QCD and λ_a ($a = 1, \dots, 8$) are the SU(3) Gell-Mann matrices. Finally $F_{\mu\nu}^a = \partial_\mu A_\nu^a - \partial_\nu A_\mu^a - gf_{bc}^a A_\mu^b A_\nu^c$ is the gluon field strength tensor, f_{abc} are the SU(3) structure constants. Note that μ, ν are the space-time indices while a, b, c denote the color indices (for more details see Ref [1]).

Now if we rewrite the quark part of the QCD Lagrangian in terms of the left and right quark fields ψ_L, ψ_R as,

$$\mathcal{L}_q = \bar{\psi}_{Lf} i\cancel{D} \psi_{Lf} + \bar{\psi}_{Rf} i\cancel{D} \psi_{Rf} - (\bar{\psi}_{Lf} m_f \psi_{Rf} + \bar{\psi}_{Rf} m_f \psi_{Lf}) - \frac{1}{4} F_{\mu\nu}^a F_a^{\mu\nu} \quad (2.2)$$

It can be seen that the mass term mixes the right and left handed fields. The remaining terms are dependent either on left handed fields or right handed fields alone but not both. Thus in the massless

limit the QCD interaction does not couple the right handed and left handed quarks, which can therefore transform independent of each other. Thus the QCD Lagrangian exhibits chiral symmetry in the massless limit. Now the up and down quark flavors have very small masses (approx. 5 and 10 MeV respectively) and may be considered massless in the relevant scale of QCD. Therefore we expect a symmetry in the observed spectra of hadrons - they should come in parity doublets. But this is not observed in nature. We do not observe parity pairs of nucleons. This indicates that though the QCD Lagrangian respects chiral symmetry, the QCD ground state or the QCD vacuum breaks it. Owing to the non trivial structure of the QCD vacuum the chiral symmetry is spontaneously broken, the idea pioneered by Nambu [2] and Nambu, Jona-Lasinio [3, 4] .

Now, the ground state of a system with a spontaneously broken symmetry should be infinitely degenerate. If we perform continuous symmetry operations on the non-symmetric ground state, we can generate an infinite number of such states. Each will have the same energy since the Hamiltonian is invariant to all such symmetry operations. Since in QCD we are dealing with continuous symmetries, the QCD vacuum should be infinitely degenerate. Due to spontaneous breaking of symmetry, only one of these possible states is realised and all the excited states are built on this particular state. In quantum field theory tunnelling between the various degenerate ground states is least probable since now we are dealing with an infinite number of degrees of freedom. To get a physical picture of the mechanism of spontaneous symmetry breaking it would be useful to

consider the example of a ferromagnet. If a ferromagnet is cooled beneath a critical temperature, the atomic spins are spontaneously aligned, with the magnetization pointing in a particular direction. Due to the exchange interaction, the state with spins aligned has the lowest possible energy ie. it is the ground state. The ground state is infinitely degenerate. On rotating the magnet, the magnetization will now point in a different direction. If the magnet is of finite extent, thus, we may be able to realise the different ground states by rotating the magnet. But if the magnet is of infinite extent, then rotating all the spins simultaneously to generate a new ground state, is practically impossible. Hence for someone residing within the infinite magnet, the direction of spin alignment is a done deal.

Another interesting example of spontaneous symmetry breaking is that of a superconductor. The BCS (Bardeen- Cooper - Schrieffer) theory was eminently successful in describing the phenomenon of superconductivity [5, 6]. The theory proposes a superconducting gap which separates the ground state from the higher excited states. The superconducting ground state comprises of correlated electron pairs. The pair formation occurs due to an attractive interaction between the electrons, mediated by phonons. To break up a pair, energy is needed, which characterises the gap. Now, the BCS ground state has a broken symmetry. Compared to the simple example of the ferromagnet, the symmetry broken here is much more abstract. It is the freedom in choosing the phase of the ground state wave function, which is broken in this case. The electric charge remains

no longer conserved. In order to save the conservation of electric charge, Nambu proposed the existence of symmetry restoring excitations - the Nambu - Goldstone (NG) waves [7, 8, 9]. In the case of a simple ferromagnet we can see that the symmetry restoring excitations are the familiar spin waves. In the case of a BCS superconductor the symmetry restoring NG modes are collective excitations of pairs of Bogolubov - Valatin (BV) quasi particles. Bogolubov had put forth an elegant mathematical formalism for the BCS theory (Valatin had independently developed a similar approach [11]), where, the elementary excitations above the ground state are the BV quasi particles[10]. They comprise a coherent mixture of electrons and holes and hence are not eigen states of charge. They are described by the BV equation. Nambu realised the analogy between the BV equation, which describes the quasi particle excitations in superconductors, and the Dirac equation for massive fermions. He elevated spontaneous symmetry breaking in infinite media and the restoring mechanism, to the status of a general principle. He then went on to extend this idea of spontaneous symmetry breaking to particle physics, inspired by the striking analogy between the BV quasiparticles and the massive Dirac fermions. His model developed together with G. Jona-Lasinio, the Nambu-Jona-Lasinio (NJ) model, puts forth the following correspondences - Free electron \leftrightarrow bare Fermion, the energy gap \leftrightarrow the Dirac mass, electric charge \leftrightarrow chirality [3, 4]. Though the dirac particle in question was the nucleon in the NJ model, it is easy to apply the correspondence to the realm of quarks. The ground state or the QCD vacuum can be con-

sidered as a condensate of quark- antiquark cooper pairs of chirality zero (ie. a pair consisting of a right handed quark and a left handed anti-quark or the other way around). Such a pair condensate implies a broken chiral symmetry, since, for such a pair, independent right handed or left handed chiral transformations are impossible. Now, breaking such a quark - anti quark cooper pair would result in a massive quark and an anti quark. Any change in the distribution of the pairs would give rise to the Nambu - Goldstone modes which try to restore the broken symmetry. The theory requires the NG modes to have spin zero and negative parity, thus suggesting the pion which possesses the requisite quantum numbers. Though the NG modes are massless excitations the pions have mass. This is because quarks possess a small but finite 'current' mass (acquired by the Higgs mechanism), which explicitly breaks the symmetry of the Lagrangian, thereby rendering the NG modes massive.

It is expected that at high temperatures/ high densities, with the formation of deconfined QGP, the broken chiral symmetry is restored and the quarks regain their current mass. There is continuing lack of clarity regarding the order of the deconfining and chiral symmetry restoring transitions. In the following section, we give a time line of the QCD phase diagram. We shall discuss the prevailing opinions regarding the ordering of deconfinement and chiral symmetry restoration.

2.2 The time line of QCD phase diagram

The possible phase transition from hadronic matter to quark gluon plasma was originally suggested by Cabibbo and Parisi, Collins and Perry [12, 13]. The earliest phase diagram of QCD matter as it appeared in the work by Cabibbo and Parisi is shown in Fig(2.1). The

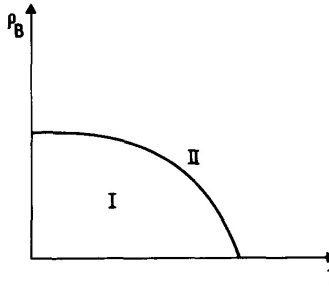


Figure 2.1: The naive phase diagram of QCD matter, with I indicating the confined hadronic phase and II, the deconfined QGP phase, which appeared in the seminal work by Cabibbo and Parisi.

diagram suggests a phase transition to quark gluon plasma both at high temperatures and low baryon densities, low temperatures and high baryonic densities. The suggestion was made based on the quark model of hadrons, with hadrons as color singlet - confined - states of the more fundamental quarks, together with the phenomenon of asymptotic freedom. Asymptotic freedom is the QCD property owing to which quarks interact weakly at close proximity, giving rise to the deconfinement transition.

A more complex phase diagram for QCD matter was conceived by G.Baym [14] a few years later and is given in Fig(2.2).

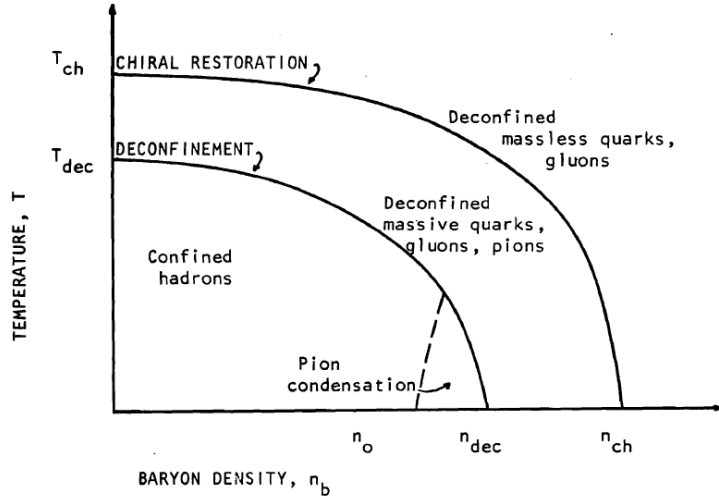


Figure 2.2: A more complex phase diagram for QCD matter conceived by G.Baym in 1982

The diagram indicates that at low temperatures and baryon densities, strongly interacting matter is in the confined hadronic phase with pionic excitations. A transition from bulk hadronic matter to a pion condensed phase is envisaged to occur at almost twice the nuclear saturation density. Again there is the evident transition to the deconfined phase of massless quarks and gluons at very high temperatures or baryon densities. The core feature of the phase diagram is an intermediate region of massive quarks, just after the deconfinement curve, preceding the region of deconfined massless quarks and gluons. In this region chiral symmetry remains spontaneously broken rendering the quarks massive.

With data flowing in from the heavy-ion collider experiments and lattice QCD simulations, the phase diagram has evolved over time. A recent QCD phase diagram by Fukushima and Hatsuda [15] (see Figure(2.3)) summarises our current understanding of the var-

ious phases of hadronic matter, obtained via the heavy ion collider experiments/ lattice QCD. The diagram also features some of the newly conjectured phases.

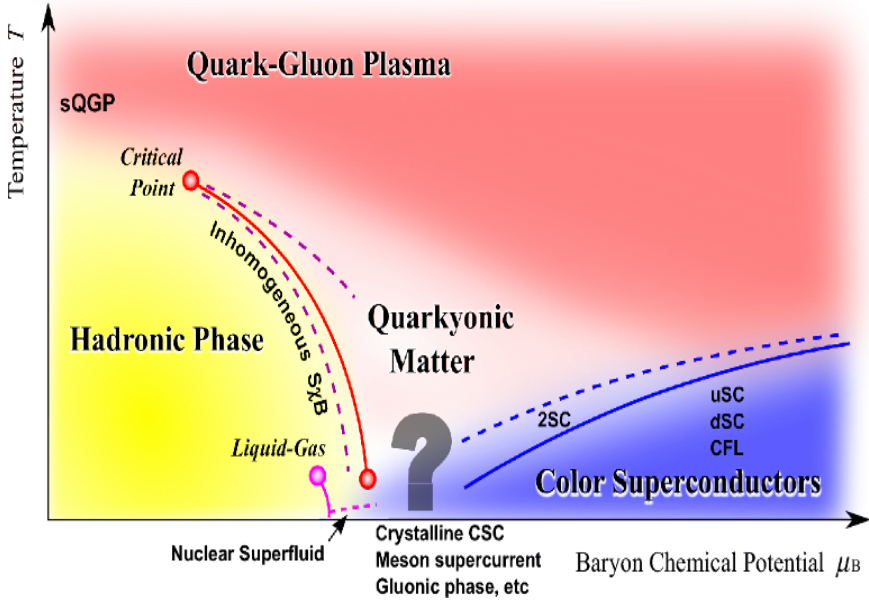


Figure 2.3: A recent QCD phase diagram by Fukushima and Hatsuda

In the phase diagram at zero baryon density there appears no boundary line separating the hadronic and QGP phase. This indicates that there is no rapid phase transition to QGP phase in this region. Rather there occurs a non singular cross over. The information comes from extensive studies carried out using numerical calculations on the lattice at finite temperature. At zero baryon density the transition properties are found to depend on the quark flavors and masses. Calculations carried out on the lattice using physical masses for quarks indicates a non singular cross over rather than a rapid phase transition [16].

Lattice data has also given information regarding the ordering of the deconfinement and chiral symmetry restoration transitions. A phase transition is generally indicated by a discontinuous change in some physical quantity, which serves as the order parameter for the transition. The quantity which serves as the order parameter for the spontaneous breaking of chiral symmetry is the chiral condensate. For the deconfinement transition the order parameter is the Polyakov loop. Polyakov loop is a gauge invariant quantity in finite temperature QCD which corresponds to the free energy of an isolated static quark. It can be simply thought of as the world line of an isolated static quark. It is called a loop since it is closed owing to the periodicity in Euclidean time. The expectation value of the Polyakov loop ($\langle P \rangle$) is related to free energy of an isolated (static) quark (F_q) as [17]

$$\langle P \rangle = e^{-F_q/T} \quad (2.3)$$

In the confined phase the free energy of an isolated quark would be infinite. Therefore the expectation value of the Polyakov loop, $\langle P \rangle$, would be zero in the confined phase. On the other hand in the deconfined phase the free energy of an isolated quark would have a finite value. Thus $\langle P \rangle$ would be non zero in the deconfined phase.

Thus we have the following conditions which determine the deconfinement and chiral symmetry restoration transitions. For the chiral symmetry broken phase, chiral condensate, $\langle q\bar{q} \rangle \neq 0$. For

the chirally symmetric phase, chiral condensate, $\langle q\bar{q} \rangle = 0$. For the quark confining phase, expectation value of the Polyakov loop, $\langle P \rangle = 0$. For the quark deconfined phase, expectation value of the Polyakov loop, $\langle P \rangle \neq 0$.

The chiral condensate vanishes exactly only when the chiral symmetry is exact. This is so if the quark masses are precisely zero. Also in the case of deconfining transition, the expectation value of the Polyakov loop vanishes only if the quark masses are infinite (static quarks). Thus for quarks with physical masses none of the above order parameters can serve as tell-tale signature of an exact critical point for the phase transition. Still it is reasonable to define a pseudo critical point in temperature, T_p , using the peak positions of the susceptibilities of order parameters. Since there are two order parameters, one concerning the deconfinement and the other, chiral symmetry restoration, two such pseudo critical points may be expected. However lattice calculations indicate that the peaks of chiral and Polyakov loop susceptibilities match [18, 19]. Therefore for physical quark masses there is a simultaneous cross over to a deconfined, chiral symmetric phase. The pseudo critical temperature lies within the range 150-200 MeV. A simple analytic description of the cross over region remains elusive since the system is still strongly correlated. A plasma of weakly coupled quarks and gluons is expected only at much higher temperatures. Nowadays the term strongly coupled quark gluon plasma (sQGP) is used to label the QCD state near the cross over temperature.

At finite chemical potential, lattice QCD runs into difficulty due

to the famous 'sign problem'. The problem arises because, at finite μ_q , the action that defines the theory becomes complex. The Boltzmann factor which serves as the statistical weight thereby becomes complex which spoils a probabilistic interpretation. Thus presently, lattice QCD can give reliable results only if the condition $\frac{\mu_q}{T} \ll 1$ is met. In the region where lattice QCD fails, effective models are employed to study the phase diagram. The method of study relies on models which are able to provide a reasonable description of hadronic properties in the vacuum. Such models are extended to the finite T/μ regime. Investigations using effective models in the region of finite chemical potential, reveals a QCD critical point [20, 21, 22, 23], for realistic u,d,s quark masses, as depicted in Figure(2.3). At the QCD critical point the chiral transition is no more a cross over but a first order transition. The QCD critical point, if it exists, should appear on the hadronic to QGP transition boundary at baryo chemical potential $\sim 100 - 500 MeV$. The region corresponds to that reached in heavy ion collisions at center of mass energies $\sim 5 - 50 GeV/u$. There is an avid search for the critical point at the detectors, PHENIX and STAR, at RHIC.

The phase diagram by Fukushima and Hatsuda displays an intermediate phase, the so called 'quarkyonic' matter, between quark gluon plasma and the confined hadronic phase. Such an intermediate phase has been proposed to exist in the large N_c limit (N_c denoting the number of color charges) [24]. Taking the large N_c limit gives a theory which is more tractable and mathematically simpler. Recent computer simulations indicate that the thermody-

namic predictions of the theory (in the large N_c limit), closely match the predictions in the real world of the three color charges [25]. In the large N_c limit confinement persists to arbitrary densities (The critical temperature, T_c for deconfinement, is found to be independent of the baryo chemical potential). The theory in this limit therefore predicts a novel phase, the quarkyonic matter, which is a confined phase at arbitrarily high densities. Quarkyonic matter lies in a density regime with baryo chemical potential, $\mu_B > M$, M being the mass of the nucleon, at temperatures less than the critical temperature for deconfinement ($T < T_c$). In such a regime the densities are high enough such that the hadrons (essentially baryons) overlap substantially. The situation therefore demands the use of the notion of a quark Fermi sea instead of a baryon Fermi sea. But there is something more to the picture. Though deep within the Fermi sea the behaviour of quarks is more or less ideal due to Pauli blocking, at the surface they show non-perturbative behaviour, in the limit of large N_c . The bulk properties of quarkyonic matter such as pressure, entropy are determined by the weakly coupled quarks within the Fermi sea. Near the Fermi surface the quarks interact strongly, whereby physical excitations on top of the Fermi surface are dominated by color singlet mesons and baryons. Whether quarkyonic matter has any existence in the real world of $N_c = 3$ remains an open question. Again the chiral transition in quarkyonic matter is highly speculative. Further in depth studies augmented by computational techniques and experiments are expected to give a conclusive answer.

Next we consider the phase diagram in the region of asymptotically high densities/ low temperatures. At these high densities quarks are weakly coupled owing to asymptotic freedom. Each quark finds in its vicinity a number of other quarks, thereby losing its sense of belonging to a particular baryon. Due to many body effects the long range confining forces are screened, leading to deconfinement. The deconfined and essentially free quarks form a Fermi sea of filled states at low enough temperatures. But even a small attractive interaction between quarks near the Fermi surface can dramatically alter the ground state. Any arbitrarily small interaction between fermions lead to Cooper pair formation, near the Fermi surface [5], leading to a superconducting phase. The ground state of the superconducting phase which is a condensate of Cooper pairs is lower in energy compared to the simple Fermi sea, and is hence a favoured state [6]. In the case of electrons which are fermions the fundamental interaction is repulsive. Pairing is hence mediated by the background lattice via phonons. In the case of quarks in the high density regime, the quark-quark interactions can be approximated by single gluon exchange interaction. Single gluon exchange is apparently attractive in the antisymmetric anti-triplet channel. Hence quark - quark Cooper pairs are formed near the Fermi surface which then grow into a condensate. Since the quark pairs have color the condensate breaks the local SU(3) color symmetry and the gluons acquire a mass. The name color - superconductivity is used to describe the phenomenon [26, 27, 28, 29]. Color superconducting quark matter can form different possible phases depending on the

pairing pattern of the quarks. At the highest densities, with quark matter composed of three massless flavors, the suggested pairing phase is the color - flavor locked (CFL) phase [30]. In the color - flavor locked phase the color and flavor symmetries become correlated. The resulting condensate is invariant only under simultaneous transformations in color and flavor space. This locking together of color and flavor breaks the chiral symmetry. The locking of left handed and right handed flavors to color would in turn lock them into each other. Thus the chiral symmetry which requires that the left handed and right handed quarks transform independent of each other, remains broken (Here therefore the phenomenon of chiral symmetry breaking occurs not due to the presence of the conventional chiral condensate. The condensate is expected to vanish at such asymptotic densities). Now, it should be noted that the calculation of the superconducting gap using perturbation theory is valid only in the limit of very high densities. Actually the calculations are performed in the regime where the chemical potential could be as high as 10^8 MeV. At moderate densities the pairing patterns are unknown though there are various possible suggestions which still remain inconclusive.

In the region of extremely low temperatures and moderately high densities, various competing exotic phases are suggested, but the picture is still vague (see the question mark denoting the region in the phase diagram Fig(2.3)). Compact star interiors are expected to fall into this region of the phase diagram. In this thesis we explore this region of the phase diagram in an attempt to develop an equa-

tion of state for cold dense matter expected to exist within compact stars. Our line of approach is as follows - within compact stars, if the deconfined quark phase exists, then the stellar matter would constitute quark matter in bulk. A look into the plasma properties of the bulk QGP phase would indeed be rewarding. It should be noted that even at the hottest temperatures achieved at the LHC, the QGP formed is not an ideal gas but is in a strongly coupled phase. Hence under realistic densities (of the order of a few times the normal nuclear density), that exists within a compact star, it is plausible that the quark matter is a strongly coupled plasma. Following this line of thought we try and estimate the coupling strength of QGP existing at the relevant densities. For the purpose, we define a plasma parameter, analogous to that for a degenerate non-relativistic QED plasma. The analogy with degenerate non-relativistic QED plasma is justified and discussed in the following chapter, where the analogy is made full use of in developing an equation of state for QGP at the relevant compact star densities. Similar work, utilizing the analogy with QED plasma, has been carried out at finite temperatures and a remarkably good fit to lattice results has been obtained earlier [31, 32]. It should be emphasized that in this thesis work we have ignored cooper instability and the attendant color superconducting phase, since the nature of pairing at densities relevant to compact stars is still a debated issue.

References

- [1] K. Yagi, T. Hatsuda, Y. Miake (2005) Quark-gluon plasma: From big bang to little bang. (Vol.23) Cambridge University Press.
- [2] Y. Nambu Unpublished talk in Broken Symmetry: Selected Papers of Y. Nambu edited by T. Eguchi and K. Nishijima (World Scientific, 1995), pp. 110126.
- [3] Y. Nambu, G. Jona-Lasinio (1961) Phys. Rev. 122, 345.
- [4] Y. Nambu, G. Jona-Lasinio (1961) Phys. Rev. 124, 246.
- [5] L.N. Cooper (1956) Phys. Rev. 104, 1189.
- [6] J. Bardeen, L.N. Cooper, and J.R. Schrieffer (1957) Phys. Rev. 106, 162; (1957) Phys. Rev. 108, 1175.
- [7] Y. Nambu (1960) Phys. Rev. 117, 648.
- [8] J. Goldstone (1961) Nuovo Cimento 19, 154.
- [9] J. Goldstone, A. Salam, S. Weinberg (1962) Phys. Rev. 127, 965.
- [10] N. N. Bogolubov (1947) J. Phys. Vol. 11, No.1, 2332.

- [11] J. G. Valatin (1958) *Nuovo cimento* 7, 843 .
- [12] N.Cabibbo and G.Parisi (1975) *Physics Letters B*, 59, 67-69.
- [13] J. C.Collins and M. J.Perry (1974) *Phys. Rev. Lett.*, 34, 1353-1356.
- [14] G.Baym, in *Quark Matter and Heavy Ion Collisions*, H Satz (Ed.), World Scientific, Singapore 1982.
- [15] K.Fukushima and T.Hatsuda (2011) *Reports on Progress in Physics*, 74, 014001.
- [16] Y Aoki et al. (2006) *Nature*, 443(7112), 675-678.
- [17] L. D.McLerran and B.Svetitsky (1981) *Physical Review D*, 24(2), 450.
- [18] F. Karsch and E. Laermann (1994) *Phys. Rev. D*50 6954.
- [19] S. Aoki, M. Fukugita, S. Hashimoto, N.Ishizuka, Y. Iwasaki, K. Kanaya, K. Kuramashi, H. Mino, M. Okawa, A. Ukawa and T. Yoshie (1998) *Phys. Rev. D*57 3910.
- [20] A.Masayuki and Y.Koichi (1989) *Nuclear Physics A*, 504(4), 668-684.
- [21] A.Barducci, R.Casalbuoni, S.De Curtis, R.Gatto and G.Pettini (1990) *Physical Review D*, 41(5), 1610.
- [22] F.Wilczek (1992) *Int. J. Mod. Phys. A*7 3911-3925.
- [23] J. Berges and K. Rajagopal (1999) *Nucl. Phys. B*538 215-232.

- [24] L. McLerran and R. D. Pisarski (2007) Nucl. Phys. A796 83-100.
- [25] M. Panero (2009) Phys. Rev. Lett. 103, 232001.
- [26] B.C. Barrois (1977) Nucl. Phys. B129, 390.
- [27] D. Bailin and A. Love (1982) Nucl. Phys. B205, 119.
- [28] M. Alford, K. Rajagopal, and F.Wilczek (1998) Phys. Lett. B 422, 247.
- [29] R. Rapp, T. Schafer, E. V. Shuryak, and M. Velkovsky (1998) Phys. Rev. Lett. 81, 53.
- [30] M. Alford, K. Rajagopal, F. Wilczek (1999) Nucl. Phys. B 537, 443.
- [31] V.M. Bannur (1999) Eur. Phys. J. C 11, 169.
- [32] V.M. Bannur (2006) J. Phys. G, Nucl. Part. Phys. 32, 993.

Chapter 3

The equation of state for QGP

within a quark star and the

Mass-Radius relationship

3.1 Introduction

Quantum Chromodynamics (QCD), the theory of strong interactions, endows hadrons with two essential features - color confinement and spontaneous chiral symmetry breaking. At sufficiently high temperatures and/or densities, QCD predicts that both these features come to an end and hadronic matter undergoes a transition to a plasma of deconfined massless quarks and gluons (chiral symmetry is restored). Whether the chiral symmetry restoration and deconfinement transition coincide or if the latter precedes the former still remains an open question. An intermediate phase of deconfined but massive quarks is therefore a possibility and has been

suggested and discussed previously by several authors [1, 2, 3, 4, 5]. Lattice calculations show that at or near $\mu = 0$, as the critical temperature T_c is reached, color deconfinement and chiral symmetry restoration occur simultaneously [6]. Now the remaining possibility is the existence of the intermediate plasma of massive quarks in the low temperature, high density limit. The intermediate phase in this limit has been discussed by Satz et al. [7], wherein the quarks are massive, dressed by a gluonic cloud. As the temperature approaches T_c , the gluonic cloud evaporates (equivalent to vanishing of the chiral condensate at T_c), leaving point like quarks and gluons. Using percolation arguments they have calculated the baryon density threshold for chiral symmetry restoration to be about 3.9 times that for color deconfinement. Compact star interiors are natural candidates where the intermediate phase could be present since the limiting conditions of high density and low temperature are met there. In this thesis we model this possible phase of QGP and develop an equation of state in the relevant density regime. The procedure is surprisingly simple. At the range of density in question the quark-quark interaction is color coulombic. There is a well established mathematical machinery, already in place, for analysing QED plasma under similar electric charge interactions. By exploiting this analogy and incorporating the requisite modifications (arising due to new internal degrees of freedom), the equation of state for QCD matter is developed. We start by estimating the coupling strength of QGP at densities relevant to compact stars, drawing analogy from conventional one component plasma (OCP). Once we have the equa-

tion of state, it is checked whether it is able to give bound quark stars with mass radius relationship typical to compact stars.

3.2 Coupling strength and equation of state of QGP

Plasma is a statistical system of mobile charged particles interacting via the electromagnetic forces . In a conventional model the electrical neutrality of the system is maintained by imbedding the charged particles in a uniform background of neutralizing charges. The plasma parameter Γ is defined as the ratio of average coulomb energy to average kinetic energy and gives the strength of coupling due to coulomb interaction. For $\Gamma \sim 1$ it is a strongly coupled plasma (SCP).

For a system of charged particles obeying classical statistics the kinetic energy maybe estimated approximately as T , where T is the absolute temperature. For a degenerate electron system with number density n one instead uses the Fermi energy

$$E_F = \frac{\hbar^2}{2m} (3\pi^2 n)^{\frac{2}{3}} \quad (3.1)$$

The plasma parameter is then estimated as

$$\Gamma = \frac{e^2/a}{E_F} = 0.543 r_s \quad (3.2)$$

where

$$a = (3/4\pi n)^{1/3} \quad (3.3)$$

is the usually referred to as the *ion-sphere radius* or the *Wigner-Seitz radius* and

$$r_s = \left(\frac{3}{4\pi n}\right)^{\frac{1}{3}} \frac{me^2}{\hbar^2} \quad (3.4)$$

is the Wigner- Seitz radius of the electrons in units of the bohr radius. For valence electrons in metals $r_s = 2 - 6$, so that the plasma parameter Γ is greater than unity and hence is a typical example of strongly coupled plasma.

The analogy is carried on to QGP : QGP expected to be found in compact stars can be regarded as a deconfined quasi-color-neutral-system of quarks and gluons with color coulombic mutual interactions. In the compact star interior it is appropriate to take the approximation $T = 0$. Hence it is plausible that quark matter in compact star interior is similar to a degenerate electron system except for a few modifications due to color degrees of freedom. In analogy with QED plasma we define the plasma parameter for QGP as

$$\Gamma = \frac{Cg_s^2/4\pi a}{E_F} \quad (3.5)^1$$

Here g_s denotes the strong charge related to the strong coupling constant by $\alpha_s = g_s^2/4\pi$. C is the color Casimir factor associated with gluon emission from a quark which is $4/3$.

Therfore in the QGP case

$$\Gamma = \frac{4\alpha_s/3a}{E_F} = 0.543r_s \quad (3.6)$$

¹In the QCD case Lorentz-Heaviside units are used.

where

$$a = (3g_c/4\pi n_f)^{1/3} \quad (3.7)$$

and

$$r_s = \left(\frac{3g_c}{4\pi n_f}\right)^{\frac{1}{3}} \frac{4M_q\alpha_s}{3} \quad (3.8)$$

g_c incorporates the color degrees of freedom, n_f stands for the number density corresponding to the particular flavor and M_q denotes the quark constituent mass.

Thus for quark matter composed of u and d quarks, with typical values $M_q \simeq m_p/3$, $\alpha_s \approx 0.5$, for densities ranging from $3\rho_0 - 10\rho_0$ (Normal nuclear density $\rho_0 = 0.16 fm^{-3}$), we obtain $r_s = 0.67 - 1$ and $\Gamma \approx 0.36 - 0.55$. Hence we have intermediate to strongly coupled QGP (SCQGP) in compact stars. Also corresponding to the scaling factor - Bohr radius - in the electron case (eqn(3.4)), we now have $(\frac{4M_q\alpha_s}{3})^{-1} \sim 1 fm$, the hadron radius.

Asymptotic formulae for the ground state energy of an assembly of electrons, imbedded in a continuum of positive charge, are known in the high and low density regimes. At high densities the limiting unperturbed state is that of a perfect Fermi gas. As the density decreases exchange terms and electron correlations of various orders become important. The resultant expansion for the ground state (in Rydbergs) in the high density (small r_s) regime, due to Gellmann and Brueckner [8] gives :

$$\begin{aligned} E_G \sim & 2.21r_s^{-2} - 0.916r_s^{-1} + 0.0622 \ln r_s - 0.096 \\ & + rs(0.0049 \ln r_s + C) + \dots \quad (3.9) \end{aligned}$$

where $C \simeq -0.02$.

In the low density (large r_s) regime the asymptotic expansion for ground state energy of the electron lattice with suitable correction terms due to Carr, Coldwell-Horsefall and Maradudin [9] gives :

$$E_G = -1.79186r_s^{-1} + 2.638r_s^{-3/2} - 0.73r_s^{-2} + \dots \quad (3.10)$$

Isihara and Montroll interpolated these two asymptotic expansions through the method of Pade approximants [10]. We use the resulting formula in the QGP case with appropriate modifications primarily with r_s given by eqn(3.8) (For a systematic discussion of the technique of two point pade approximation see appendix 1 of reference [10]). The general formula for the ground state energy per quark (in MeV) :

$$\left(\frac{9}{8M_q\alpha_s^2}\right)\frac{d^2E_G}{dr^2} = \frac{13.26 + 1.7085r_s^{1/2} - 1.8144r_s - 0.3813r_s^{3/2} - 0.1011r_s^2 + 0.0121r_s^{5/2} + 0.0099r_s^3}{1 + 0.1288r_s^{1/2} + 0.0013r_s - 0.0110r_s^{3/2} - 0.0028r_s^2} \quad (3.11)$$

Therefore for quark matter composed of u and d quarks the total energy density is given by,

$$\epsilon_G = \sum_{f=1}^2 n_f E_{Gf} + B \quad (3.12)$$

and the corresponding pressure,

$$P = \sum_{f=1}^2 \left(-\frac{n_f r_{sf}}{3}\right) \frac{\partial E_{Gf}}{\partial r_{sf}} - B \quad (3.13)$$

Where B denotes the confinement parameter in the form of MIT bag constant.

For typical densities at the core in the SCQGP model, the quark chemical potential $\mu_q \simeq 400 MeV$. This lies below the strange quark

constituent mass which is in the range $m_s \simeq 0.5 - 0.6$ GeV [11].

This justifies the exclusion of strange quarks in the model.

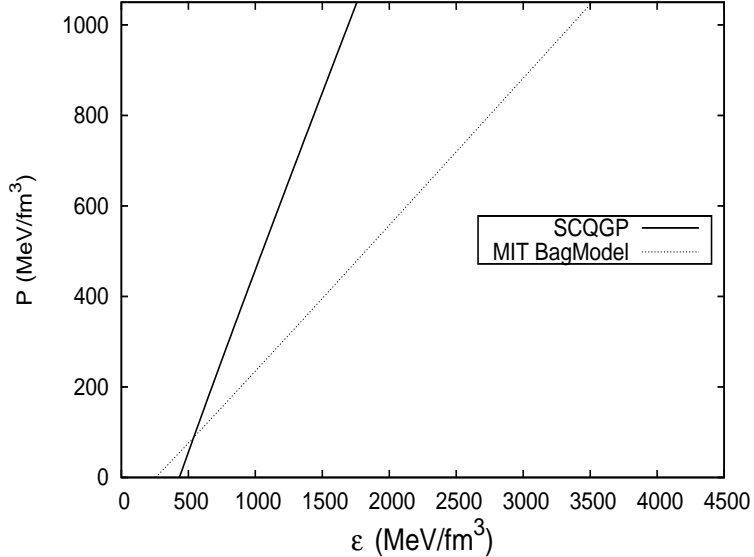


Figure 3.1: Equations of state for quark matter - solid line: SCQGP EOS evaluated for $B^{1/4} = 200$ MeV, dashed line: MIT BagModel EOS for non-interacting quarks with $m_u = m_d = 0, m_s = 150$ MeV and $B^{1/4} = 145$ MeV.

In Figure 3.1, the SCQGP EOS for quark matter evaluated for $B^{1/4} = 200$ MeV (solid line) is shown together with the EOS for non-interacting quarks within the MIT BagModel (dashed line). We have taken $m_u = m_d = 0, m_s = 150$ MeV and $B^{1/4} = 145$ MeV. The interactions between the quarks in the SCQGP case has rendered the EOS stiffer as compared to the non-interacting case. Next we check whether the new equation of state can give bound stars with observed mass-radius relations.

3.3 The mass - radius relationship

For a spherically symmetric system the space-time metric has the form

$$ds^2 = e^{2\nu} dt^2 - e^{2\lambda} dr^2 - r^2(d\theta^2 + \sin^2 \theta d\phi^2), \quad (3.14)$$

where r and t are the radial and time coordinates respectively, θ and ϕ are the respective angles and ν, λ the metric functions.

The energy-momentum tensor for a perfect fluid is given by

$$T^{\mu\nu} = (\epsilon + P)u^\mu u^\nu + pg^{\mu\nu} \quad (3.15)$$

Here u^μ is the local fluid four-velocity, $u^\mu = \frac{dx^\mu}{ds}$ and p, ϵ are the pressure and energy density in the rest frame of the fluid.

When the star is in a state of hydrostatic equilibrium, the Einstein field equations, given the space-time metric (3.14) and the energy momentum tensor (3.15), yield the equations of structure known as the Tolman-Oppenheimer-Volkoff equations [12, 13]

$$\frac{dp}{dr} = -\frac{[p(r) + \epsilon(r)][m(r) + 4\pi r^3 P(r)]}{r[r - 2m(r)]} \quad (3.16)$$

$$m(r) = 4\pi \int_0^r \epsilon(r')r'^2 dr' \quad (3.17)$$

Here m is the *included mass* within the coordinate r . Now, with Eqs.(3.12) and (3.13) we solve the TOV equations and obtain the mass-radius relations for quark stars.

The SCQGP equation of state suggests stable stars (Fig: 3.2 & 3.3 - solid lines) with mass-radius typical to compact stars. In Figure 3.2 the M-R relations obtained for the SCQGP case are com-

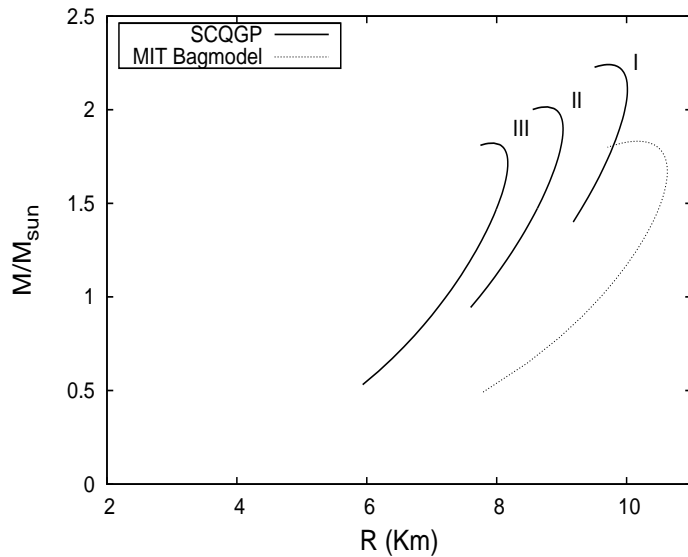


Figure 3.2: Mass- radius relationship for quark stars - solid lines: SCQGP EOS labelled I, II & III corresponding to values of confinement parameter $B^{1/4} = 200, 210$ and 220 MeV, respectively; dashed line: non-interacting quarks with $m_u = m_d = 0, m_s = 150$ MeV within the MIT BagModel, $B^{1/4} = 145$ MeV.

pared with that for non-interacting quarks within the MIT Bagmodel. With $B^{1/4}=145$ MeV the non-interacting case yields maximum mass star with mass $1.83M_{\odot}$. In the SCQGP case strong coupling between quarks and the possible massive quark phase, stiffened the equation of state to yield stable sequences with maximum mass $\gtrsim 2M_{\odot}$ for $B^{1/4} \lesssim 215$ MeV. Recently the mass of the binary millisecond pulsar J1614-2230 has been calculated to high accuracy using Shapiro delay, to be $1.97 \pm 0.04 M_{\odot}$ [14]. The discovery constrains softer equations of state with corresponding maximum mass star $< 2M_{\odot}$. The SCQGP EOS is however in conformity with the recent discovery for appropriate choice of bag parameter values.

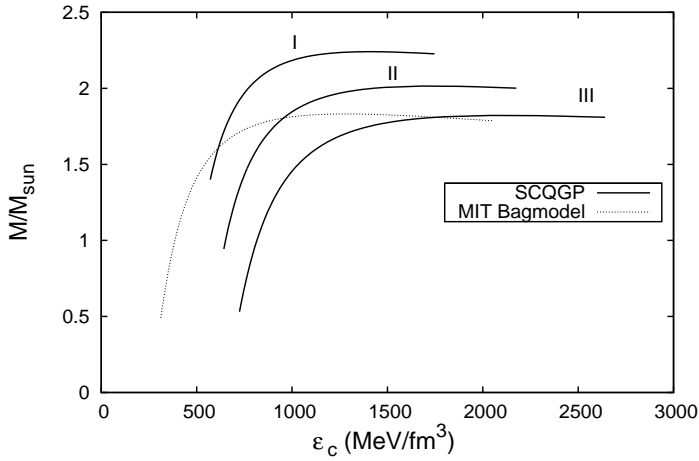


Figure 3.3: Mass sequences - solid lines: SCQGP EOS with I, II, III - corresponding to values of confinement parameter $B^{1/4} = 200, 210$ and 220 MeV, respectively; dotted line: Non-interacting quarks with $m_u = m_d = 0, m_s = 150$ MeV within the MIT BagModel, $B^{1/4} = 145$ MeV.

We summarize our results in the table below :

Table 3.1: The limiting mass (M_{max}) of quark stars in the SCQGP model for different B values. The corresponding radius (R), central energy density (ϵ_c) and quark number density (n_c) are given

| $B^{1/4}$ MeV | M_{max} M_\odot | R Km | ϵ_c GeV/fm 3 | n_c fm $^{-3}$ |
|------------------|------------------------|-----------|-----------------------------|---------------------|
| 200 | 2.241 | 9.72 | 1.411 | 5.15 |
| 210 | 2.015 | 8.78 | 1.682 | 5.65 |
| 220 | 1.822 | 7.96 | 2.043 | 6.30 |

We make the following conclusions : quark matter at relevant densities inside a compact star is intermediately to strongly coupled (SCQGP). The equation of state of a degenerate electron system obtained via Pade approximation yields a similar EOS for QGP, *mutatis mutandis*. On solving the TOV equations with the resultant equation of state, we obtain stable stars with mass-radius typical to compact stars . For $B^{1/4} \lesssim 215$ MeV, the stiff equation of state gives stable sequences with maximum mass $\gtrsim 2M_\odot$. The result conforms to recent observations.

References

- [1] E.V Shuryak, Phys.lett. **107B** (1981)103.
- [2] R.Pisarski, Phys.Lett. **110B** (1982)155.
- [3] G.Baym, *in Quark Matter and Heavy Ion Collisions*, ed. by H.Satz (World Scientific, Singapore, 1982).
- [4] J.Cleymans, K.Redlich, H.Satz, E.Suhonen, Z.Phys.C **33** (1986) 151.
- [5] H.Schulz and G.Röpke, Z.Phys.C **35** (1987) 379.
- [6] A.Bazavov et al., Phys.Rev.D **80** (2009) 014504.
- [7] P.Castorina, R.V.Gavai, H.Satz, Eur.Phys.J C, **69**, (2010) 169.
- [8] M.Gell-Mann, and K. Brueckner, Phys.Rev.106, 394 (1987).
- [9] W.J.Carr, Jr.,Phys.Rev.122, 1437 (1961); R.A Coldwell-Horsefall and A.A Maradudin, Phys.Rev.1, 395 (1960).
- [10] A.Ishihara and E.W.Montroll, Proc.Nat.Acad.Sci.(USA) 68, 3111 (1971).
- [11] K.Steininger, W.Weise, Phys.Lett.B329 (1994), 169.
- [12] R.C. Tolman, Phys. Rev.55, 364-373 (1939).
- [13] J.R.Oppenheimer and G.M Volkoff, Phys.Rev. 55, 374 (1939).

[14] P.B.Demorest et al. *Nature* 467, 1081 (2010).

Chapter 4

Radial oscillations and stability of quark stars with strongly coupled QGP in their interior

4.1 Introduction

The pioneering work of Chandrasekhar[1, 2] in the framework of general relativity revealed the existence of a dynamical instability, wherein gaseous masses become unstable with respect to radial pulsations well before the Schwarzschild limit is reached. His conclusion defines the sufficiency condition for the stability of a compact star - that it should be able to withstand small radial perturbations (The necessary condition being $\frac{\partial M(\epsilon_c)}{\partial \epsilon_c} > 0$, M being the equilibrium stellar mass and ϵ_c the central energy density). In the previous chapter we have developed the SCQGP equation of state describing matter within cold, pure quark stars composed of massive and strongly

coupled quarks. From the mass sequences, obtained employing the equation of state, the necessary condition for stability is found to be satisfied (see Fig(3.3)). To check the sufficiency condition, the normal mode analysis of radial oscillations has to be carried out. The radial pulsations that preserve the spherical symmetry of a star do not result in the emission of gravitational radiation. Hence the normal mode analysis of such oscillations is less complicated and straightforward. The eigenequation of Chandrasekhar which governs the normal modes has the Sturm-Liouville form. The eigenmodes hence constitute a complete set and any arbitrary periodic radial motion can be expressed as their superposition.

Studies on radial pulsations of quark stars – hypothetical stars with quark matter in the interior – have been carried out earlier by a number of authors for different proposed equations of state for dense quark matter (For e.g. [3], [4], [5], [6], [7]). Here we start by analysing the radial oscillations of quark stars described by the SCQGP equation of state. We calculate the oscillation periods of the fundamental and first overtone for different values of the confining bag parameter (B). The eigen functions of the lowest three normal radial modes are then analysed, for the particular example of $B^{1/4} = 210\text{MeV}$. We then go on and study the damping of pulsations due to non-equilibrium processes. The corresponding neutrino emissivities are derived and the temporal evolution of pulsation energies are analysed. For illustration, calculations are performed for SCQGP stars with bag value, $B^{1/4} = 210\text{MeV}$ and the results are plotted for stellar masses $1.518, 1.845, 2M_{\odot}$.

4.2 Normal radial modes of quark stars in the SCQGP model

When a compact star is in a state of hydrostatic equilibrium, the Einstein field equations, given the space-time metric (3.14) and the energy momentum tensor (3.15), yield the equations of structure known as the Tolman-Oppenheimer-Volkoff equations [8, 9]

$$\frac{dm}{dr} = 4\pi r^2 \epsilon, \quad (4.1)$$

$$\frac{dp}{dr} = -\frac{(p + \epsilon)(m + 4\pi r^3 p)}{r(r - 2m)}, \quad (4.2)$$

$$\frac{d\nu}{dr} = -\frac{1}{p + \epsilon} \frac{dp}{dr}, \quad (4.3)$$

Here m is the *included mass* within the coordinate r . The metric function λ is given by

$$e^{2\lambda} = (1 - \frac{2m}{r})^{-1} \quad (4.4)$$

λ has the same form both inside and outside the star although it is the included mass m and not the total mass that appears in the interior solution. In order to match the exterior Schwarzschild solution the metric function ν should obey the boundary condition $\nu(r = R) = \frac{1}{2} \ln(1 - \frac{2M}{r})$, where M is the mass of the star and R its radius.

The equations governing radial oscillations were originally obtained by Chandrasekhar[1, 2] on perturbing the equilibrium con-

figurations governed by equations (4.1)-(4.3) in a manner such that the spherical symmetry is not violated and only the terms linear in order are retained. In our discussion we denote the normal mode motions of the star by $\delta r(r, t) = \xi_n(r)e^{i\omega_n t}$. Here $\xi_n(r)$ are the normal mode amplitudes (or ‘eigenfunctions’) of the n th normal mode, $n=0$ being the fundamental or nodeless mode. The quantities ω_n are the radial eigenfrequencies of the perturbed star.

Employing a new variable $u_n = r^2 e^{-\nu} \xi_n$, the Chandrasekhar eigenequation governing the radial modes appears in the the Sturm-Liouville form

$$\frac{d}{dr} \left(P \frac{du_n}{dr} \right) + (Q + \omega_n^2 W) u_n = 0 \quad (4.5)$$

The functions $P(r)$, $Q(r)$ and $W(r)$ expressed in terms of equilibrium configurations of the star are given by

$$\begin{aligned} P &= e^{(\lambda+3\nu)} r^{-2} \gamma p, \\ Q &= -4e^{(\lambda+3\nu)} r^{-3} \frac{dp}{dr} - 8\pi e^{3(\lambda+\nu)} r^{-2} p(\epsilon + p) \\ &\quad + e^{(\lambda+3\nu)} r^{-2} (\epsilon + p)^{-1} \left(\frac{dp}{dr} \right)^2, \\ W &= e^{(3\lambda+\nu)} r^{-2} (\epsilon + p), \end{aligned} \quad (4.6)$$

Here $\gamma = \frac{(\epsilon + p)}{p} \frac{dp}{d\epsilon}$ denotes the adiabatic index. Solutions to the eigenequation are physically acceptable only if they satisfy certain boundary conditions. At the center of the star the requirement that δr and $\frac{d\delta r}{dr}$ are finite there leads to the condition

$$\frac{u_n}{r^3} \text{ should be finite or zero as } r \rightarrow 0 \quad (4.7)$$

At the surface of the star the Lagrangian change in pressure, Δp should vanish which leads to the condition

$$\Delta p = -\frac{\gamma p e^\nu}{r^2} \frac{du_n}{dr} = 0 \quad \text{at } r = R. \quad (4.8)$$

The eigenequation can now be solved using standard procedure to obtain the frequency spectrum ω_n^2 ($n = 0, 1, 2, \dots$) of the normal modes. The squared normal mode frequencies being eigenvalues of the Sturm-Liouville equation are real and form an infinite discrete sequence, $\omega_0^2 < \omega_1^2 < \omega_2^2 < \dots$. For a star to be stable against radial perturbations ω^2 should be positive since then ω itself is real. If any of the eigenvalues, ω^2 , is negative then ω would be purely imaginary leading to a solution that grows exponentially as $e^{|\omega|t}$. Thus a negative value of ω^2 indicates instability. Since the frequencies increase sequentially with n , $\omega_0^2 > 0$ is the sufficient condition for stability.

The eigenmode analysis performed employing the equation of state for SCQGP with different values for the confinement parameter B , yields the spectrum of eigenfrequencies, ω_n^2 . The squared frequencies ω_0^2 go to zero as the maximum mass star is reached, as expected. We have plotted the results obtained by the normal mode analysis in Fig.(4.1) and Fig.(4.2).

Solid lines indicate the period ($\tau_n = 2\pi/\omega_n$) calculated for the SCQGP equation of state for different B values ($B^{1/4} = 190, 200, 210 MeV$). Dotted lines indicate the period calculated for strange stars composed of non-interacting quarks with $m_u = m_d = 0, m_s = 150 MeV$

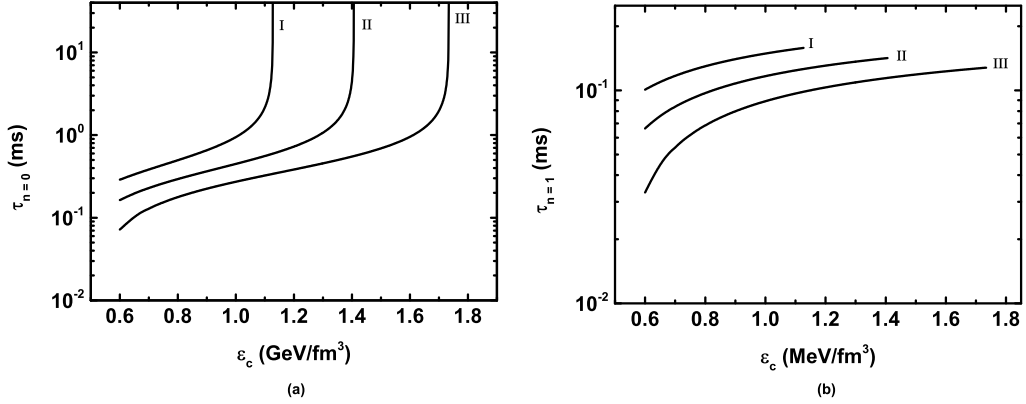


Figure 4.1: (a),(b)-Oscillation periods (τ), calculated for the SCQGP EOS, as a function of central energy density (ϵ_c) for the fundamental and first excited modes respectively. The curves are labelled I,II & III corresponding to values of confining bag parameter $B^{1/4} = 190, 200 \& 210 MeV$ in order.

within the MIT Bag Model for $B^{1/4} = 145 MeV$, which we have plotted for comparison. Figures (4.1a), (4.1b) show the variation in period with central energy density (ϵ_c) for the fundamental and first excited modes respectively. The resulting pattern of curves indicates that for a particular value of ϵ_c , of the various mass sequences obtained for different values of the bag constant, if we pick the more massive star - it has a higher value of pulsation period . It is found that pulsation periods tend to zero as the central density approaches its minimum possible value, a property characteristic to quark stars as opposed to hadronic stars [4]. The Fig(4.2a) shows the period as a function of the stellar mass M (in units of solar mass) for the fundamental radial mode ($n=0$). It is found that for lower mass stars the pulsation periods of the fundamental mode are typically of the order of one tenth of a millisecond and have negligible dependence on the bag parameter. For medium and higher mass stars a variation

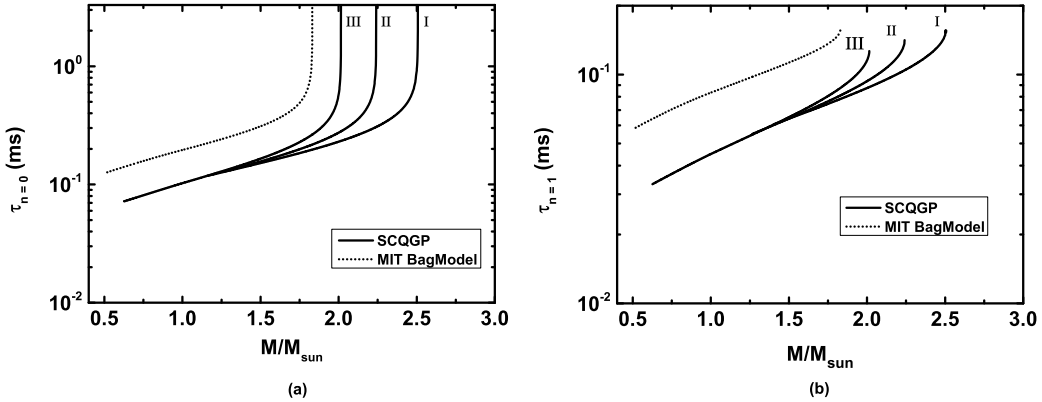


Figure 4.2: (a),(b)-Oscillation periods as a function of mass M for the fundamental and first excited modes respectively. Solid lines represent the period calculated for the SCQGP EOS and are labelled I,II & III corresponding to values of confinement parameter $B^{1/4} = 190, 200 \& 210\text{MeV}$ respectively. Dotted lines indicate the period obtained for strange stars composed of non-interacting quarks with $m_u = m_d = 0, m_s = 150\text{MeV}$ within the MIT BagModel for $B^{1/4} = 145\text{MeV}$.

of pulsation periods with change in the confining bag parameter(B) is seen - the periods show a decrease with decrease in bag constant. The behaviour may be explained by noting that the stiffness of the equation of state tends to increase with decrease in the confining bag constant. Thus for quark stars of the same mass decreasing B value indicates a stronger coupling between the quark constituents which increases the normal mode frequencies/ lowers the pulsation periods. The behaviour is more pronounced in the case of intermediate to higher mass stars. Comparing with strange stars composed of non-interacting quarks with $m_u = m_d = 0, m_s = 150\text{MeV}$ treated within the MIT Bag model with bag constant $B^{1/4} = 145\text{MeV}$ we see that the oscillation periods show considerable difference throughout the entire range of stellar masses with the difference increasing

with decrease in bag parameter value (increasing stiffness) for the SCQGP equation of state. For SCQGP stars the oscillation periods are 2 to 3 times lower than that for strange stars with non-interacting quarks for the chosen bag constants (In earlier work by [10], [11] a similar difference was seen in the case of hadronic stars with and without interaction). In Fig(4.2b) we have plotted the pulsation periods for the first excited mode ($n=1$) as a function of stellar mass M again for SCQGP stars as well as for strange stars within the non-interacting bag model. For the first excited mode the pulsation periods have typical values in the range, approx. $1/2 - 1/3$ that of the fundamental mode. The distribution of curves follow the pattern akin to that of the fundamental mode discussed above, with the compared difference with the non-interacting model now relatively less.

4.3 Normal mode eigenfunctions of the radial modes and the energy stored in the pulsations

A careful study of the behaviour of the normal mode amplitudes with radial distance r provides insight into how matter described by a particular equation of state responds to radial perturbations. The normal mode amplitudes of radial oscillations are given by the eigenfunctions, $\xi_n(r)$, of the Sturm-Liouville equation (eqn.(4.5)). We now examine the variation of the normal mode amplitudes with radius r , by plotting and analysing the eigenfunctions, $\xi_n(r)$ for strongly coupled quark matter. The eigenfunctions are normalized

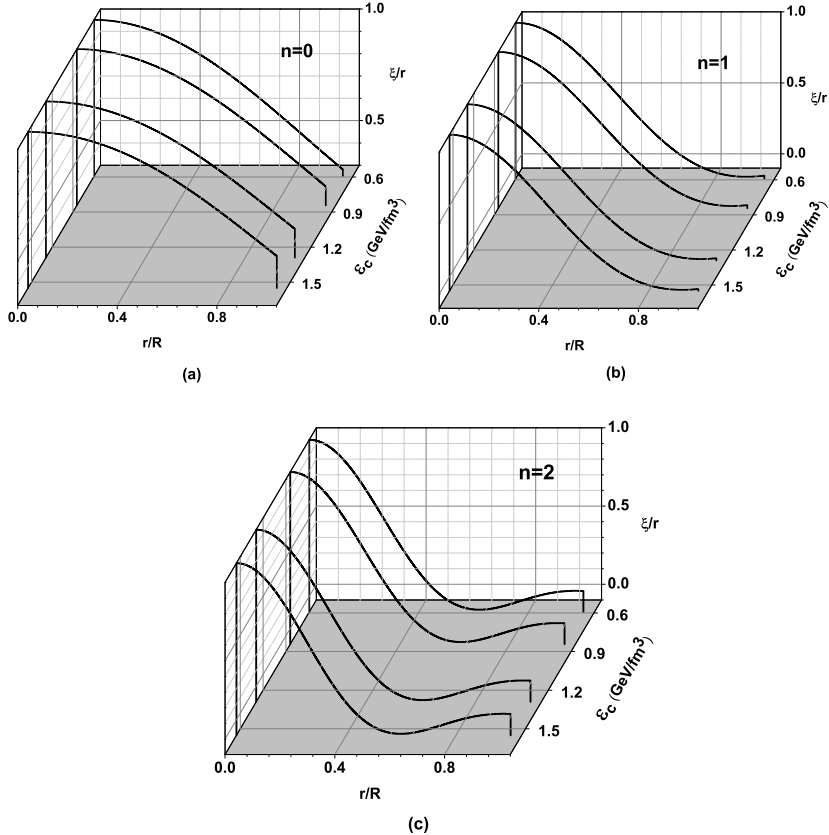


Figure 4.3: The ‘relative eigenfunctions’ ξ/r , for the SCQGP equation of state, plotted against the ‘relative radius’ r/R , for central energy densities $\epsilon_c = 0.6, 0.84, 1.3$ and 1.55 GeV/fm^3 and bag parameter $B^{1/4} = 210 \text{ MeV}$. Fig(4.3a) represents the fundamental mode ($n=0$). Fig(4.3b) and Fig(4.3c) represent the first ($n = 1$) and second ($n = 2$) excited modes respectively.

using the condition

$$\lim_{r \rightarrow 0} \frac{\xi_n}{r} = \Delta \quad (4.9)$$

Δ is a small normalization parameter. For illustration we choose the bag parameter as $B^{1/4} = 210 \text{ MeV}$. Since it allows for a better comparison the ‘relative eigenfunctions’ ξ_n/r are plotted against ‘relative radius’ r/R , R being the radius of the star. The typical

eigenfunctions for the fundamental ($n = 0$), first excited ($n = 1$) and second excited ($n = 2$) modes, with normalization parameter $\Delta = 1$, are shown in Fig(4.3), each for central energy densities $\epsilon_c = 0.6, 0.84, 1.3$ and $1.55 \text{ GeV}/\text{fm}^3$. The corresponding stars have masses $0.56, 1.65, 1.98, 2.01 M_\odot$ respectively. For the fundamental mode the relative amplitude deviates from the homologous behaviour ($\xi/r = 1$) starting from the core and continues to decrease with an increasing slope towards the outer layers of the star. The shapes of the normal mode amplitudes tend to be determined by the degree of homogeneity of the stellar model. The fundamental mode is approximately homologous only if the logarithm of energy density ($\log_{10}\epsilon$) and the adiabatic index (γ) are roughly constant throughout the configuration barring the outermost layers [11]. In the current model both $\log_{10}\epsilon$ and γ are found to vary throughout the star. The variation in γ is more striking. In Fig(4.4) a plot of the adiabatic index as a function of energy density is shown.

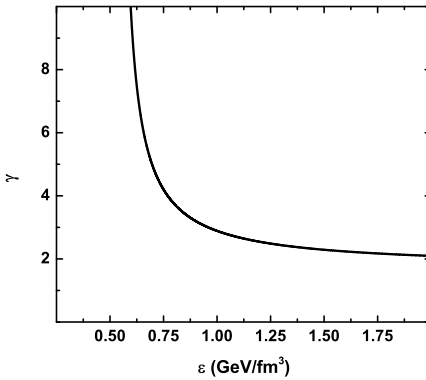


Figure 4.4: The variation in the adiabatic index γ with energy density ϵ for the SCQGP equation of state with bag parameter $B^{1/4} = 210 \text{ MeV}$

The adiabatic index is found to increase first slowly and then

steeply with decreasing energy density. The behaviour of the adiabatic index can be attributed to the stiffness of quark matter due to strong coupling between quarks as well as the effect of the bag. With increasing adiabatic index the compressibility of matter decreases thereby accounting for the steady decrease in ξ/r . The fundamental mode is hence found to be much sensitive to changing adiabatic index. Though not so evident, on careful examination it is seen that there is a slight increase in the relative amplitude of the fundamental mode with increasing central density as we move towards the maximum mass star. The relative eigenfunctions of the first and second excited modes show sinusoidal behaviour but with increasingly smaller values in the outer layers of the star.

Once the spatial distribution of normal mode amplitudes $\xi_n(r)$ are given, the pulsation energy stored in the radial oscillations can be computed. Just like an arbitrary pulsation can be expressed as a superposition of the normal modes, so the pulsation energy can be written in terms of the normal mode components [11]

$$E_{puls} = \sum_n A_n^2 E_{puls}^{(n)} \quad (4.10)$$

$$\text{with } E_{puls}^{(n)} = 2\pi\omega_n^2 \int_0^R W(r^2 e^{-\nu} \xi_n)^2 dr \quad (4.11)$$

The function $W(r)$ is given by eqn(4.6). The dimensionless amplitudes A_n can be determined from pulsation damping mechanisms which operate to dissipate the energy stored in the pulsations. We consider the damping of radial pulsations and the resultant temporal evolution of pulsation energy in the next section. We restrict

our calculations to small amplitude pulsations ($\Delta \ll 1$) and for illustration choose the bag parameter value $B^{1/4} = 210 \text{ MeV}$.

4.4 Damping of pulsations by non-equilibrium processes

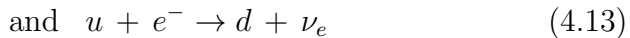
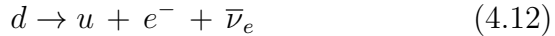
For a non-vibrating quark star with matter described by the zero temperature SCQGP equation of state, the condition for β equilibrium is given by the relation¹, $\delta\mu = \mu_d - \mu_u - \mu_e = 0$. Here μ_i are the chemical potentials of the particle species u , d and e^- . Radial pulsations drive the stellar matter out of chemical equilibrium in which case $\delta\mu(r, t) \neq 0$. The processes tending to restore the matter back to equilibrium lead to the damping of pulsations. The most efficient of the non-equilibrium processes is the direct-Urca process. The direct-Urca processes are simple β -decay processes which in the case of ordinary neutron star matter are the reactions $n \rightarrow p + e^- + \bar{\nu}_e$ and $p + e^- \rightarrow n + \nu_e$. In ordinary neutron stars the direct-Urca process is forbidden since the laws of conservation of momentum and energy cannot be satisfied for the expected composition of neutron star matter. On the other hand the analogous processes can occur for quark matter - the energy and momentum conservation laws are satisfied once we take into consideration the the finite quark masses and/or the interaction between quarks [12]. In the SCQGP phase we have assumed the quarks to be massive and interacting. Hence we

¹Here we consider quark matter to be composed of u,d quarks and electrons such that conditions of β -equilibrium and charge neutrality are satisfied. In the original SCQGP EOS, the contribution due to electrons was ignored since the corresponding modification to the EOS is negligible at quark matter densities.

expect direct-Urca process to be the primary and dominant source of pulsation damping in such quark stars.

In what follows we analyse the quark direct-Urca process in the domain of SCQGP model and calculate the associated neutrino luminosities. Initially we consider the general case of a vibrating quark star at finite temperature T . In this connection we closely follow Iwamoto[12, 13] while making appropriate modifications pertinent to the context. Iwamoto has derived the neutrino luminosities for equilibrium quark matter at finite T which we adapt to the non-equilibrium case.

For quark matter devoid of strange quarks the direct-Urca process is given by the reactions



The rate at which energy is lost due to neutrino emission process (4.12) in a unit volume, the neutrino emissivity, is given by

$$\begin{aligned} \varepsilon_{\bar{\nu}_e}(T, \delta\mu) &= 6V^{-1} \left(\prod_{i=1}^4 V \int \frac{d^3 p_i}{(2\pi)^3} \right) E_2 \\ &\times W_{fi} n(\vec{p}_1) [1 - n(\vec{p}_3)] [1 - n(\vec{p}_4)] \end{aligned} \quad (4.14)$$

W_{fi} is the transition rate for β -decay given by

$$W_{fi} = V (2\pi)^4 \delta^4(p_1 - p_2 - p_3 - p_4) |M|^2 / \prod_{i=1}^4 2E_i V \quad (4.15)$$

where the four-vectors, $p_i = (E_i, \vec{p}_i)$, numbered from $i = 1$ to 4, de-

note the particles $d, \bar{\nu}_e, u, e^-$ in order. The factor 6 stands for the three color and two spin degrees of freedom of the initial d quark, V represents the normalization volume and $n(p_i) = (1 + \exp[(E_i - \mu_i)/kT])^{-1}$ is the Fermi-distribution function. The term $(1-n(p))$ ensures that the exclusion principle is obeyed. $|M|^2$ is the squared invariant amplitude averaged over initial d quark spin (σ_1) and summed over the final spins of u quark (σ_3) and electron (σ_4),

$$|M|^2 = \frac{1}{2} \sum_{\sigma_1, \sigma_3, \sigma_4} |M_{fi}|^2 = 64 G^2 \cos^2 \theta_c (p_1 \cdot p_2)(p_3 \cdot p_4) \quad (4.16)$$

where the weak-coupling constant, $G \simeq 1.435 \times 10^{-49}$ erg cm³ and θ_c is the Cabibbo angle ($\cos^2 \theta_c \simeq 0.948$). In the SCQGP model u and d quarks are massive and non-relativistic while electrons are ultra-relativistic. We therefore have

$$(p_1 \cdot p_2)(p_3 \cdot p_4) \simeq E_1 E_2 E_3 E_4 \left(1 - \frac{|\vec{p}_3|}{E_3} \cos \theta_{34} \right) \times \left(1 - \frac{|\vec{p}_1|}{E_1} \cos \theta_{12} \right) \quad (4.17)$$

with $\cos \theta_{ij} = \vec{p}_i \cdot \vec{p}_j / |\vec{p}_i| \cdot |\vec{p}_j|$. In degenerate Fermi systems only those particles with momenta that lie close to the respective Fermi surfaces can participate in a reaction. Hence we can replace the magnitude of quark and electron momenta by the respective Fermi momenta. Accordingly $\cos \theta_{34}$ can be expressed as a function of Fermi-momenta ($p_F(i)$) of the involved fermions. We neglect the neutrino momentum in our calculations. The integrals in the ex-

pression for emissivity can now be decoupled and one can write

$$\varepsilon_{\bar{\nu}_e}(T, \delta\mu) = \frac{24G^2 \cos^2 \theta_c}{(2\pi)^8} \left(1 - \frac{p_F(u)}{m_u^*} \cos \theta_{34}\right) A B \quad (4.18)$$

m_i^* denotes the quark effective mass, $i = d, u$. Here

$$A = \left(\prod_{i=1}^4 \int d\Omega_i \right) \delta^3(\vec{p}_1 - \vec{p}_3 - \vec{p}_4) \left(1 - \frac{|\vec{p}_1|}{E_1} \cos \theta_{12} \right) \quad (4.19)$$

is an angular integral and

$$\begin{aligned} B = & p_F(d) p_F(u) p_F^2(e) m_d^* m_u^* \int_0^\infty dE_1 \int_0^\infty E_2^2 dE_2 \\ & \times \int_0^\infty dE_3 \int_0^\infty dE_4 E_2 S \delta(E_1 - E_2 - E_3 - E_4) \end{aligned} \quad (4.20)$$

is the energy integral with $S = n(\vec{p}_1)(1 - n(\vec{p}_3))(1 - n(\vec{p}_4))$. The angular integral can be done analytically to give $A = 32\pi^3 / p_F(d) p_F(u) p_F(e)$.

The energy integral can be evaluated using standard procedure and

can be written, in terms of dimensionless variables $y = E_2/kT$ and

$\delta\bar{\mu} = \delta\mu/kT$ as

$$B = p_F(d) p_F(u) p_F^2(e) m_d^* m_u^* \frac{(kT)^6}{2} F(\delta\bar{\mu}) \quad (4.21)$$

The dimensionless function F is defined as

$$F(x) = \int_0^\infty y^3 dy \left(\frac{\pi^2 + (y-x)^2}{1 + \exp(y-x)} \right) \quad (4.22)$$

Next we consider the limiting case in which $\delta\bar{\mu} \gg 1$. Then the function F can be represented by the asymptotic formula $F \approx (1/60)(\delta\bar{\mu})^6$ [14]. If we finally write down the neutrino emissivity

in this particular limiting case $\delta\bar{\mu} \gg 1$, we obtain the temperature independent form

$$\begin{aligned}\varepsilon_{\bar{\nu}_e}(\delta\mu) &= \frac{G^2 \cos^2 \theta_c}{40\pi^5 \hbar^{10} c^4} p_F(e) m_d^* m_u^* \\ &\times \left(1 - \frac{p_F(u)}{m_u^* c} \cos \theta_{34}\right) (\delta\mu)^6\end{aligned}\quad (4.23)$$

This final equation for neutrino emissivity is what we need in our specific case of a zero temperature pulsating SCQGP quark star. Following the same method we can calculate the ν_e emission rate from the inverse process (4.13) which yields the same expression as the above in the limiting case $-\delta\bar{\mu} \gg 1$. In this latter limiting condition the inverse process of ν_e emission (4.13) dominates over the $\bar{\nu}_e$ emission process (4.12)(which is then negligible in comparison). In the former limit the converse is true. It has to be pointed out that during our calculation of neutrino emissivities we naively replace the quark effective masses by their constituent masses. To obtain an expression for the Fermi momenta ($p_F(q)$) of strongly coupled degenerate quarks we have utilised the formula for Fermi momentum derived in the case of an electron fluid with Coulomb interactions by Isihara & Kojima [15]. Appropriate modifications are done to include the quark color degrees of freedom primarily by replacing r_s for degenerate electron system by r_s for degenerate, massive quarks given by eqn(3.8). In natural units we can write

$$p_F(q) = \frac{8}{3} M_q \alpha_s \left(\frac{0.95957}{r_s} A(r_s) \right) MeV \quad (4.24)$$

with $A(r_s) = 1 - 0.16586 r_s + r_s^2 (0.0084411 \ln r_s - 0.027620)$

To proceed with our analysis of pulsation damping we next write down the relationship between the chemical potential difference $\delta\mu(r, t)$ and an arbitrary pulsation $\xi(r, t)$. The relation has been derived in the context of neutron β -decay [16], but can be readily applied to quarks which possess a baryon number. The relation is as follows

$$\delta\mu(r, t) = -\frac{\partial\delta\mu(n_b, x_e)}{\partial n_b} n_b \frac{e^\nu}{r^2} \frac{\partial}{\partial r} (r^2 e^{-\nu} \xi(r, t)) \quad (4.25)$$

Here the partial derivative with respect to n_b is taken at constant $x_e = n_e/n_b$. The variables n_b , n_e are the equilibrium baryon number density, electron number density respectively. Using the above equation we can express the neutrino emissivities in terms of $\xi(r, t)$. If we denote the total neutrino emissivity by $\varepsilon = \varepsilon_\nu + \varepsilon_{\bar{\nu}}$, then the total redshifted neutrino luminosity L of the star is given by

$$L = \int_0^R \bar{\varepsilon} e^{2\nu} dV \quad (4.26)$$

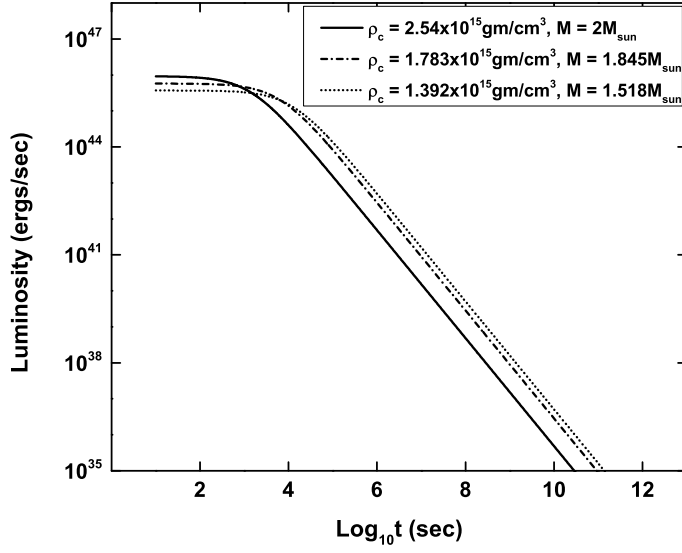
where $\bar{\varepsilon}$ is the total neutrino luminosity averaged over a pulsation period and dV is the proper volume, $dV = 4\pi r^2 e^\lambda dr$.

We now go forth and calculate the pulsation damping in the fundamental mode of a zero temperature SCQGP quark star. In the presence of pulsation damping the normal mode motions can be represented by, $\xi_0(r, t) = A_0(t) \xi_0(r) \cos \omega t$. The dimensionless amplitude $A_0(t)$ is a slowly decreasing function of time with $A_0(t = 0) = 1$. The pulsation energy in the fundamental mode with damping is $E_{puls} = E_{puls}^{(0)} A_0^2(t)$. Now assuming the direct-Urca reactions to be the only major damping mechanism present,

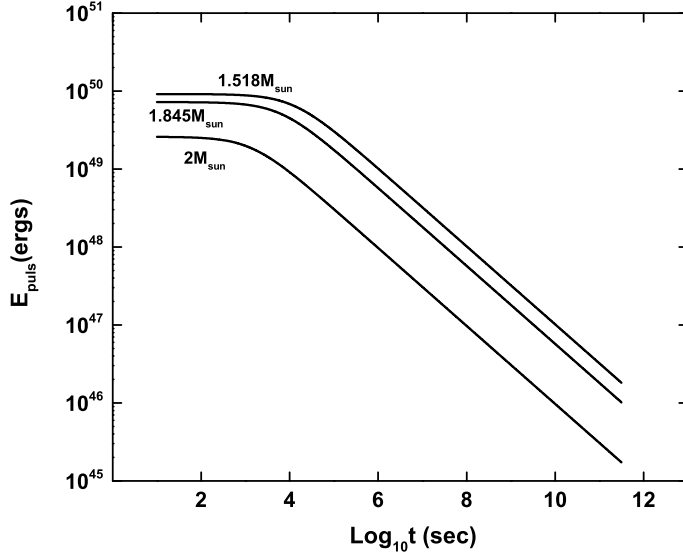
the rate of energy loss from pulsations is equal to the total neutrino luminosity:

$$-\frac{dE_{puls}}{dt} = L \quad (4.27)$$

On solving the above equation with the initial condition $A_0(0) = 1$, we obtain the variation in pulsation energy with time. We have calculated the neutrino luminosities and pulsation energies in the fundamental mode for SCQGP quark stars for the bag parameter $B^{1/4} = 210 \text{ MeV}$ and normalization parameter $\Delta = 0.01$. The chosen central densities are $\rho_c = 1.392 \times 10^{15}$, 1.783×10^{15} , $2.54 \times 10^{15} \text{ gm cm}^{-3}$ which yield stars of masses 1.518 , 1.845 , $2M_\odot$ respectively. The corresponding neutrino luminosities are plotted in Fig(4.5a) as a function of time, t . The variation in pulsation energies with time is shown in Fig(4.5b). The figure demonstrates that the capacity of higher mass quark stars, to store the pulsation energy is much less than that of lower mass stars. Lower mass stars can store a relatively increased pulsation energy for longer intervals of time as compared to higher mass stars. This behaviour can be explained by noting that the pulsation energy is dependent on the square of the normal mode frequency. From earlier calculations (see figures Fig(4.1) and Fig(4.2)) it is evident that the normal mode frequencies of quark stars decrease with increase in stellar mass M . Now the rate of energy loss due to pulsation damping tapers off with time. Therefore it comes out that lower mass stars can retain higher pulsation energies for longer durations when compared to higher mass stars. The neutrino luminosities plotted in Fig(4.5a)



(a)



(b)

Figure 4.5: Fig.(4.5a) shows the neutrino luminosities (L), in the fundamental mode for SCQGP stars with bag parameter $B^{1/4} = 210\text{MeV}$, as a function of time. The chosen central densities are $\rho_c = 1.392 \times 10^{15}$, 1.783×10^{15} , $2.54 \times 10^{15} \text{ gm cm}^{-3}$ with stellar masses 1.518 , 1.845 , $2M_\odot$ respectively. The normalization parameter $\Delta = 0.01$. Fig.(4.5b) shows the temporal evolution of pulsation energy in the fundamental mode for SCQGP stars with chosen bag parameter, central densities and corresponding stellar masses as in Fig.(4.5a).

show a more dramatic behaviour. The neutrino luminosity initially follows the pattern $L_{2M_\odot} > L_{1.845M_\odot} > L_{1.518M_\odot}$. In a matter of hours this pattern is found to be reversed. The baryon number density ($n_b(r)$) of higher mass quark stars have values larger compared to their lower mass counterparts. Hence the moment the damping is ‘switched on’, the number of triggered β -reactions and the corresponding number of emitted neutrinos are far greater than that for lower mass stars - the initial pattern for luminosity results. Now the oscillation frequencies of lower mass quark stars are larger compared to higher mass quark stars. Therefore with passage of time the β -reaction rates of lower mass stars catch up with the higher mass stars which oscillate with a lower frequency. Hence a reversal of pattern results.

References

- [1] S.Chandrasekhar, Phys.Rev.Lett., **12**, (1964) 114.
- [2] S.Chandrasekhar, Astrophys.J., **140**, (1964) 417 .
- [3] O.G. Benvenuto, J.E. Horvath, Mon.Not.R.Astron.Soc., **250**, (1991) 679.
- [4] H.M.Väth, G.Chanmugam, Astron.Astrophys., **260**, (1992) 250.
- [5] O.G.Benvenuto, G.Lugones, Int. Jour. Mod. Phys. D, **7**, (1998) 29.
- [6] V.K.Gupta, V.Tuli, A.Goyal, Astrophys.J., **579**, (2002) 374.
- [7] C.V.Flores, G.Lugones, Phys.Rev.D., **82**, (2010) 063006.
- [8] R.C. Tolman, Phys. Rev.**55**, (1939) 364-373.
- [9] J.R.Oppenheimer, G.M Volkoff, Phys.Rev. **55**, (1939) 374.
- [10] S.Tsuruta, J.P.Wright, A.G.W.Cameron, Nature, **206**, (1965) 1137.
- [11] D.W.Meltzer, K.S.Thorne, Astrophys.J., **145**, (1966) 514.

- [12] N.Iwamoto, Phys. Rev. Lett., **44**, (1980) 1637.
- [13] N.Iwamoto, Ann. Phys., **141**, (1982) 1.
- [14] P.Haensel, Astron. Astrophys., **262**, (1992) 131.
- [15] A.Isihara, D.Y.Kojima, Phys. Cond. Matter, **18**, (1974) 249.
- [16] M.E.Gusakov, D.G.Yakovlev, O.Y.Gnedin, Mon.Not.R. Astron.Soc., **361**, (2005) 1415.

Chapter 5

Conclusion

We have conducted a study of dense matter at extremely low temperatures and moderate baryon densities . In this niche of the $T - \mu$ phase diagram, the nature of dense matter is not yet conclusive. Based on arguments given in section 3.1, it is quite plausible that matter in this region is in the deconfined quark phase, wherein chiral symmetry has not yet been restored. It turns out that the relevant densities are those realised by nature in compact star interiors. Hence we expect that compact stars contain quark matter in bulk, with the constituting quarks in the massive phase. Surmising that the study of bulk plasma properties of this intermediate massive phase of quark matter would be rewarding, we set up on the trail, drawing upon the analogy with the well known QED plasma. Defining the plasma parameter for a system of degenerate massive quarks at near zero temperature, in the same line as QED plasma (since in our density range of concern the quark - quark interactions are expected to be color Coulombic), the coupling strength of QGP

was calculated. It turns out that in the density range $3\rho_0 - 10\rho_0$ (Normal nuclear density $\rho_0 = 0.16\text{fm}^{-3}$), QGP is intermediately to strongly coupled (SCQGP). Next, to obtain an equation of state for the relevant QGP phase, we carried on further with the QED plasma analogy. Utilizing the equation of state of a degenerate electron system obtained via Pade approximation a similar EOS for QGP was developed, *mutatis mutandis*. Appropriate changes were made considering the relevant color and flavor degrees of freedom. Once the equation of state was in place the next task was to check whether it was able to yield stable bound stars with mass-radius typical to compact stars. The equations of structure, the Tolman-Oppenheimer-Volkoff (TOV) equations were solved with the resultant equation of state. For $B^{1/4} \lesssim 215\text{MeV}$ (B being the confining bag parameter), the stiff equation of state gives stable sequences with maximum mass $\gtrsim 2M_\odot$. The result is relevant since it is in conformity with recent observation. Recently the mass of the binary millisecond pulsar J1614-2230 has been calculated to high accuracy using Shapiro delay, to be $1.97 \pm 0.04 M_\odot$ [1]. The result constrains soft equations of state, which yield mass sequences with maximum mass star $< 2M_\odot$. The SCQGP equation of state yield mass sequences with maximum mass star $\gtrsim 2M_\odot$ for apposite choice of bag parameter values.

In order to check whether quark stars described by the SCQGP equation of state satisfy the sufficient condition for stability, a study of the radial pulsations of the corresponding quark stars was carried out. The sufficient condition for stability is that the stars be stable

with respect to radial perturbations. The normal mode analysis of the radial modes confirmed the stability of quark stars described by the new equation of state. The normal mode pulsation periods for the fundamental and first excited modes were obtained and plotted for varying bag parameter values (B). The calculated pulsation periods for the fundamental mode are typically of the order of one tenth of a millisecond. For lower mass quark stars the pulsation periods are found to have negligible dependence on the confining bag parameter value. For medium and higher mass stars a variation in oscillation periods is seen with change in the bag parameter. The periods are found to decrease with decrease in bag constant (increasing stiffness of the EOS). Furthermore we have compared the oscillation periods of SCQGP stars with strange stars composed of non-interacting quarks treated within the MIT bag model. The oscillation periods for SCQGP stars show considerable difference (2 to 3 times lower) when compared to strange stars with non-interacting quarks throughout the entire range of stellar masses with the difference increasing with decrease in bag parameter value for the SCQGP equation of state. Thus the detection of radial oscillations (if and when possible) can provide information constraining the equation of state for dense matter.

In our study we have plotted and analysed the eigenfunctions for SCQGP stars for the fundamental, first and second excited modes in the particular case of bag parameter value, $B^{1/4} = 210\text{MeV}$. A strong correlation is found between the variation in adiabatic index and behaviour of the eigenfunctions for the fundamental mode. The

adiabatic index is found to shoot up near the surface layer of the star which must be attributed to the presence of the confining bag. Hence the particular behaviour of the plotted eigenfunctions must be restricted to quark stars.

Finally we considered the damping of the radial pulsations by non-equilibrium processes. We have derived the expression for neutrino emissivity due to the major and dominant non-equilibrium process – the direct-Urca process – for small amplitude radial pulsations. The direct-Urca process is open in the interior of an SCQGP star composed of massive and interacting quarks. The derivation was done under the assumption that stellar matter is transparent to neutrinos and thereby neglecting their effect on the kinematics of the process. In the case of zero temperature SCQGP stars the formula for emissivity has a temperature independent form. The red shifted neutrino luminosities in the fundamental mode were calculated for some specific cases. We chose the bag parameter value $B^{1/4} = 210\text{MeV}$ and picked stars with masses 1.518, 1.845 and $2M_\odot$. The temporal evolution of pulsation energy in the aforesaid cases were obtained and plotted. The damping time scale is found to be of the order of years. The plots indicate that lower mass stars can store a relatively increased pulsation energy for longer intervals of time as compared to higher mass stars. Though exact calculations have not been made it may be surmised that a fraction of the energy extracted by the Urca process is converted to electron kinetic energy, heating up the star. Consequently this should lead to electro magnetic emissions from the surface of the quark star.

Future Work

In this thesis we have considered quark stars constituted entirely of pure quark matter. A more realistic version would have pure quark matter possibly confined to the core region. The outer layers would comprise a mixed phase with quarks and hadrons interspersed, in physical equilibrium with each other, followed by a hadronic crust. In future work, the study of such a more realistic ‘hybrid star’, using a modified equation of state, incorporating the new possible phases can be undertaken.

Again, in this thesis we have considered static, non- rotating quark stars. It would be worthwhile to consider the slow and fast rotation of quark stars, which affects the structure of the star as well as the space-time in its vicinity. The limits on rotation posed by mass loss at the equator can provide valuable information about the internal structure of the star. A study of gravitational instabilities arising due to rotation is also worth pursuing.

Analysis of the non-radial oscillation modes of quark stars is significant, due to the associated emission of gravitational waves. Gravitational waves travel through space-time basically unaffected, carrying ‘pure’ information regarding the physical structure of the quark star. The study of the non-radial oscillation modes can hence provide rich and valuable information concerning matter at extreme densities.

References

- [1] P.B.Demorest et al. *Nature* 467, 1081 (2010).